Orexinergic neurons in the hypothalami of an Asiatic lion, an African lion, and a Southeast African cheetah

Oddes, D., Ngwenya, A., Malungo, I. B., Burkevica, A., Hård, T., Bertelsen, M. F., Spocter, M. A., Scantlebury, D. M., & Manger, P. R. (2023). Orexinergic neurons in the hypothalami of an Asiatic lion, an African lion, and a Southeast African cheetah. *Journal of Comparative Neurology*, *531*(3), 366-389. https://doi.org/10.1002/cne.25431

Document Version:
Publisher's PDF, also known as Version of record

Queen's University Belfast - Research Portal:
Link to publication record in Queen's University Belfast Research Portal

RESEARCH ARTICLE

WILEY

Orexinergic neurons in the hypothalami of an Asiatic lion, an African lion, and a Southeast African cheetah

Demi Oddes[1] | Ayanda Ngwenya[1] | Illke B. Malungo[1] | Anita Burkevica[2] |
Therese Hård[3] | Mads. F. Bertelsen[4] | Muhammad A. Spocter[1,5] |
D. Michael Scantlebury[6] | Paul R. Manger[1]

[1]School of Anatomical Sciences, Faculty of Health Sciences, University of the Witwatersrand, Johannesburg, South Africa

[2]Parken Zoo i Eskilstuna AB, Eskilstuna, Sweden

[3]Borås Zoo, Borås, Sweden

[4]Centre for Zoo and Wild Animal Health, Copenhagen Zoo, Frederiksberg, Denmark

[5]Department of Anatomy, Des Moines University, Des Moines, Iowa, USA

[6]School of Biological Sciences, Queen's University Belfast, Belfast, UK

Correspondence
Paul Manger, School of Anatomical Sciences, Faculty of Health Sciences, University of the Witwatersrand, 7 York Road, Parktown, Johannesburg, 2193, South Africa.
Email: Paul.Manger@wits.ac.za

Abstract

Employing orexin-A immunohistochemistry, we describe the distribution, morphology, and nuclear parcellation of orexinergic neurons within the hypothalami of an Asiatic lion (*Panthera leo* subsp. *persica*), an African lion (*Panthera leo* subsp. *melanochaita*), and a Southeast African cheetah (*Acinonyx jubatus* subsp. *jubatus*). In all three felids, the clustering of large, bipolar, and multipolar hypothalamic orexinergic neurons primarily follows the pattern observed in other mammals. The orexinergic neurons were found, primarily, to form three distinct clusters—the main, zona incerta, and optic tract clusters. In addition, large orexinergic neurons were observed in the ventromedial supraoptic region of the hypothalamus, where they are not typically observed in other species. As has been observed in cetartiodactyls and the African elephant, a cluster of small, multipolar orexinergic neurons, the parvocellular cluster, was observed in the medial zone of the hypothalamus in all three felids, although this parvocellular cluster has not been reported in other carnivores. In both subspecies of lions, but not the cheetah, potential orexin-immunopositive neurons were observed in the paraventricular hypothalamic nucleus, supraoptic nucleus, the lateral part of the retrochiasmatic area, and the inner layer of the median eminence. The distribution and parcellation of orexinergic neurons in the hypothalami of the three felids studied appear to be more complex than observed in many other mammals and for the two subspecies of lion may be even more complex. These findings are discussed in terms of potential technical concerns, phylogenetic variations of this system, and potentially associated functional aspects of the orexinergic system.

KEYWORDS
Carnivora, Felidae, hypocretin, immunohistochemistry, orexin, RRID:AB_91545, stereology

1 | INTRODUCTION

Neurons that produce orexin (hypocretin) are primarily distributed within the hypothalamus (e.g., Sakurai et al., 1998; de Lecea et al., 1998). These hypothalamic orexinergic neurons send axons, with varying densities of terminal networks, throughout the entire nervous system (e.g., Nixon & Smale, 2007; Peyron et al., 1998). While considered to be involved in the regulation of sleep and wakefulness (e.g., Inutsuka & Yamanaka, 2013), orexinergic neurons also play a role in a range other functions, with an emphasis on the regulation of appetite (e.g., Kukkonen et al., 2002; Soya & Sakurai, 2020; Zhang et al., 2013). Thus, the orexinergic system appears to be involved in regulating the balance between the need to obtain nutrition and the need to sleep—if not enough nutrition has been obtained, the orexin system may play a role in maintaining arousal until the appetitive need has been met.

Orexinergic neurons have been reported primarily to form three specific clusters within the hypothalamus, a main cluster in the perifornical region, a zona incerta cluster in the dorsolateral aspect of the hypothalamus near to the zona incerta, and an optic tract cluster in the ventrolateral aspect of the hypothalamus adjacent to the optic tract (e.g., Nixon & Smale, 2007). This three-cluster organization of the orexinergic system has been observed in many mammals including the eastern gray kangaroo (Yamamoto et al., 2006); Tasmanian devil (Patzke et al., 2014); tree pangolin (Imam et al., 2019); domestic cat (Wagner et al., 2000; Zhang et al., 2001); domestic dog (Thannickal, et al., 2000); banded mongoose and domestic ferret (Pillay et al., 2017); megachiropteran bats (Dell et al., 2013); hedgehogs and shrews (Calvey et al., 2016); several species of rodents (Bhagwandin et al., 2011; Kruger et al., 2012; Nixon & Smale, 2007; Sweigers et al., 2017); cape hare and northern tree shrew (Calvey et al., 2015); three species of Strepsirrhine primate (Calvey et al., 2015); macaque monkey (Luna et al., 2017); human (e.g., Moore et al., 2001; Thannickal et al., 2000); rock hyrax (Gravett et al., 2011); and giant otter shrew, Hottentot golden mole, and four-toed sengi (Calvey et al., 2013).

Despite this organizational consistency across metatherian and eutherian mammals (orexinergic neurons in the prototherian monotremes have not yet been investigated), variations have been noted. In several species of microchiropteran bats, the orexinergic neurons of the optic tract cluster were not observed (Kruger et al., 2010). In several species of Cetartiodactyls (Iqbal et al., 2001; Ettrup et al., 2010; Dell et al., 2012; Dell, Karlsson, et al., 2016; Dell, Patzke, et al., 2016; Davimes et al., 2017; Malungo, Gravett, Bhagwandin, Davimes, & Manger, 2020) as well as the African elephant (Maseko, Patzke, Fuxe, & Manger, 2013), a novel cluster of small orexinergic neurons, termed the parvocellular cluster (Dell et al., 2012), has been observed medial to the fornix. In the lar gibbon and chimpanzee, the orexinergic neurons of the optic tract cluster have been observed to extend into the ventromedial supraoptic region (Williams et al., 2022). Lastly, in some species of rodents, potential orexinergic neurons have been observed in the paraventricular and supraoptic nucleus (Nixon & Smale, 2007).

Framed within this background of consistency and variance in the parcellation of hypothalamic orexinergic neurons across therian mammals, here we report our observations, based on immunohistochemical staining with an orexin-A antibody, on the distribution, parcellation, and number of orexinergic neurons in three large-brained Felidae—an Asiatic lion, an African lion, and a Southeast African cheetah.

2 | MATERIALS AND METHODS

2.1 | Specimens

Brains from one adult female Asiatic lion (brain mass: 184.4 g), one adult male African lion (brain mass: 166.4 g), and one adult male Southeast African cheetah (brain mass: 139.8 g) were obtained from the Parken Zoo, Sweden, the Copenhagen Zoo, Denmark, and the Borås Zoo, Sweden. All three animals were born in captivity, were healthy, and showed no behavioral problems or stereotypies indicative of any neurological impairments. The animals were treated and used according to the guidelines of the University of Witwatersrand Animal Ethics Committee, which correspond with those of the National Institutes of Health for care and use of animals in scientific experimentation. All appropriate local animal welfare legislations and governmental protocols were followed. The brains were obtained after the animals had been euthanized with sodium pentobarbital (IV) and the death was confirmed by a veterinarian, in line with population management decisions of the zoos independent of the current study (Bertelsen, 2018). Following euthanasia, the carotid arteries were cannulated, and the heads were perfused with an initial rinse of 0.9% saline solution at a temperature of 4°C followed by 4% paraformaldehyde in 0.1 M phosphate buffer (PB) at 4°C. The brains, which showed no signs of neuropathology, were removed from the skull and postfixed in 4% paraformaldehyde in 0.1 M PB (48 h at 4°C) and allowed to equilibrate in 30% sucrose in 0.1 M PB before being stored in an antifreeze solution at −20°C until use (Manger et al., 2009).

2.2 | Sectioning and immunohistochemical staining

Blocks of the hypothalamus and diencephalon were dissected from these brains and allowed to equilibrate in 30% sucrose in 0.1 M PB, and then frozen in crushed dry ice. The frozen brains were mounted to an aluminum stage and coronal sections of 50-µm thickness were cut using a sliding microtome. All brains were sectioned in a coronal plane into one in 20 series, of which two series were used in the current study. The remaining 18 series were placed in antifreeze solution and stored at −20°C for later use. The two series used in this study were stained for Nissl substance and immunostained for orexin-A (see below). Sections used for Nissl staining were mounted on 0.5% gelatin-coated glass slides, cleared in a solution of 1:1 chloroform and 100% alcohol overnight, and then the sections were stained with 1% cresyl violet. The Nissl-stained sections were used to define the architecture of the hypothalamus and surrounding structures.

The series of sections used for orexin-A immunohistochemistry were initially treated for 30 min with an endogenous peroxidase inhibitor (49.2% methanol:49.2% 0.1 M PB:1.6% of 30% H_2O_2), followed by three 10-min rinses in 0.1 M PB. The sections were then preincubated at room temperature for 3 h in a blocking buffer solution composed of 3% normal goat serum (NGS), 2% bovine serum albumin (BSA; Sigma), and 0.25% Triton X-100 (Merck) in 0.1 M PB. The sections were then placed in a primary antibody solution (blocking buffer with appropriately diluted primary antibody) and incubated at 4°C for 48 h under gentle shaking. To identify orexin-A-containing cell bodies, we used the AB3704 anti-Orexin-A rabbit polyclonal antibody from Merck-Millipore (AB3704, Merck-Millipore; RRID AB_91545; raised against a synthetic peptide corresponding to the c-terminal portion of bovine orexin-A peptide) at a dilution of 1:3000. The pattern of staining of orexinergic neurons in the hypothalamus, while showing some variance, was generally similar to that seen in other mammals (e.g., Li & Kiruoac, 2008; Dell, Karlsson, et al., 2016).

The incubation in the primary antibody solution was followed by three 10-min rinses in 0.1 M PB, after which the sections were incubated in a secondary anti-rabbit antibody solution for 2 h at room temperature. The secondary antibody solution contained a 1:1000 dilution of biotinylated anti-rabbit IgG (BA-1000, Vector Labs) in a solution containing 3% NGS and 2% BSA in 0.1 M PB. This was followed by three 10-min rinses in 0.1 M PB after which the sections were incubated in AB solution (Vector Labs) for 1 h. After three further 10-min rinses in 0.1 M PB, the sections were placed in a solution of 0.05% diaminobenzidine in 0.1 M PB for 5 min, followed by the addition of 3 µl of 30% H_2O_2 to each 1 ml of solution in which each section was immersed. Chromatic precipitation of the sections was monitored visually under a low power stereomicroscope. This process was allowed to continue until the background staining of the sections was appropriate for architectonic analysis without obscuring any immunopositive structures. The precipitation process was stopped by immersing the sections in 0.1 M PB and then rinsing them twice more in 0.1 M PB. To check for nonspecific staining from the immunohistochemistry protocol, we omitted the primary antibody and the secondary antibody in selected sections, which produced no evident staining. While no preabsorption test was conducted for the specific antibody used in the current study, this has been done previously for this antibody in the rat and blocked all staining (Nambu, Sakurai, Mizukami, Hosoya, Yanagisawa, & Goto, 1999). The immunohistochemically stained sections were mounted on 1% gelatin-coated slides and left to dry overnight. The sections were then dehydrated in graded series of alcohols, cleared in xylene, and cover slipped with Depex.

2.3 | Anatomical reconstruction and photomicrography

A low power stereomicroscope was used to examine the Nissl-stained sections and camera lucida drawings outlining architectural borders were made. The associated orexin-A-immunostained sections were matched to these drawings and the stained neurons were marked. The delineation of the various orexinergic clusters was based on clear dif-ferences in the dendritic orientations (for the main, zona incerta, and optic tract clusters), the size of the soma (for the parvocellular cluster), and the location of the orexinergic neurons (for the supraoptic cluster) (see results and figures for these details). The drawings were then scanned and redrawn using the Canvas Draw 6 drawing program (Canvas GFX, Inc., FL, USA). Digital photomicrographs were captured using an Axiocam 208 color camera mounted to a Zeiss Axioskop microscope (with Zeiss A-Plan 5×/0.12, Zeiss Plan-NeoFluar 10×/0.30, and Zeiss Plan-NeoFluar 40×/0.75 objectives). No pixelation adjustment or manipulation of the captured images was undertaken, except for the adjustment of contrast, brightness, and levels using Adobe Photoshop.

2.4 | Stereological analysis

To quantify the total numbers of orexinergic neurons in the hypothalamus of the three species studied, an unbiased design-based systematic random sampling stereological protocol was employed. We used a MicroBrightfield (MBF) (Colchester, Vermont, USA) system with a three-plane motorized stage, Zeiss.Z2 Axio Imager Vario microscope, and StereoInvestigator software (MBF, version 11.08.1; 64-bit). Initially pilot studies were conducted to optimize sampling parameters, such as the counting frame and sampling grid sizes, and achieve an appropriate coefficient of error (Gundersen, 1988; West, Slomianka, & Gundersen, 1991; Dell, Karlsson, et al., 2016). In addition, we measured the tissue section thickness at every fifth sampling site. The vertical guard zone, at both the top and bottom of the section, was determined according to tissue thickness to avoid errors/biases due to sectioning artifacts (West et al., 1991; Dell, Karlsson, et al., 2016), and stereological counts were undertaken using a 40× objective. Table 1 provides a detailed summary of the stereological parameters employed in the current study. To estimate the total number of orexinergic neurons in the standard orexinergic clusters (main, zona incerta, optic tract, and supraoptic clusters), and the parvocellular cluster, we used the optical fractionator probe (West et al., 1991; Dell, Karlsson, et al., 2016), first estimating the total number within these clusters in the right hypothalamus, and then doubling this estimate to obtain the total number of orexinergic neurons in the standard and parvocellular clusters. To determine orexinergic neuronal volumes, we used the nucleator probe, with five rays being sampled in each probe. For all tissue sampled, this probe was used concurrently with the optical fractionator while maintaining strict criteria, that is, only neurons with complete cell bodies were analyzed.

3 | RESULTS

In the current study, we employed orexin-A immunohistochemistry to reveal orexinergic neurons within the hypothalami of an Asiatic lion, an African lion, and a Southeast African cheetah. The neurons labeled with the orexin-A antibody were all found within the hypothalamus of the three felids studied and could be parcellated into several distinct clusters (Figures 1 and 2). The three typically mammalian clusters (main, zona incerta, and optic tract clusters) were noted in all three felids and encompassed the majority of the orexinergic neurons. In all three
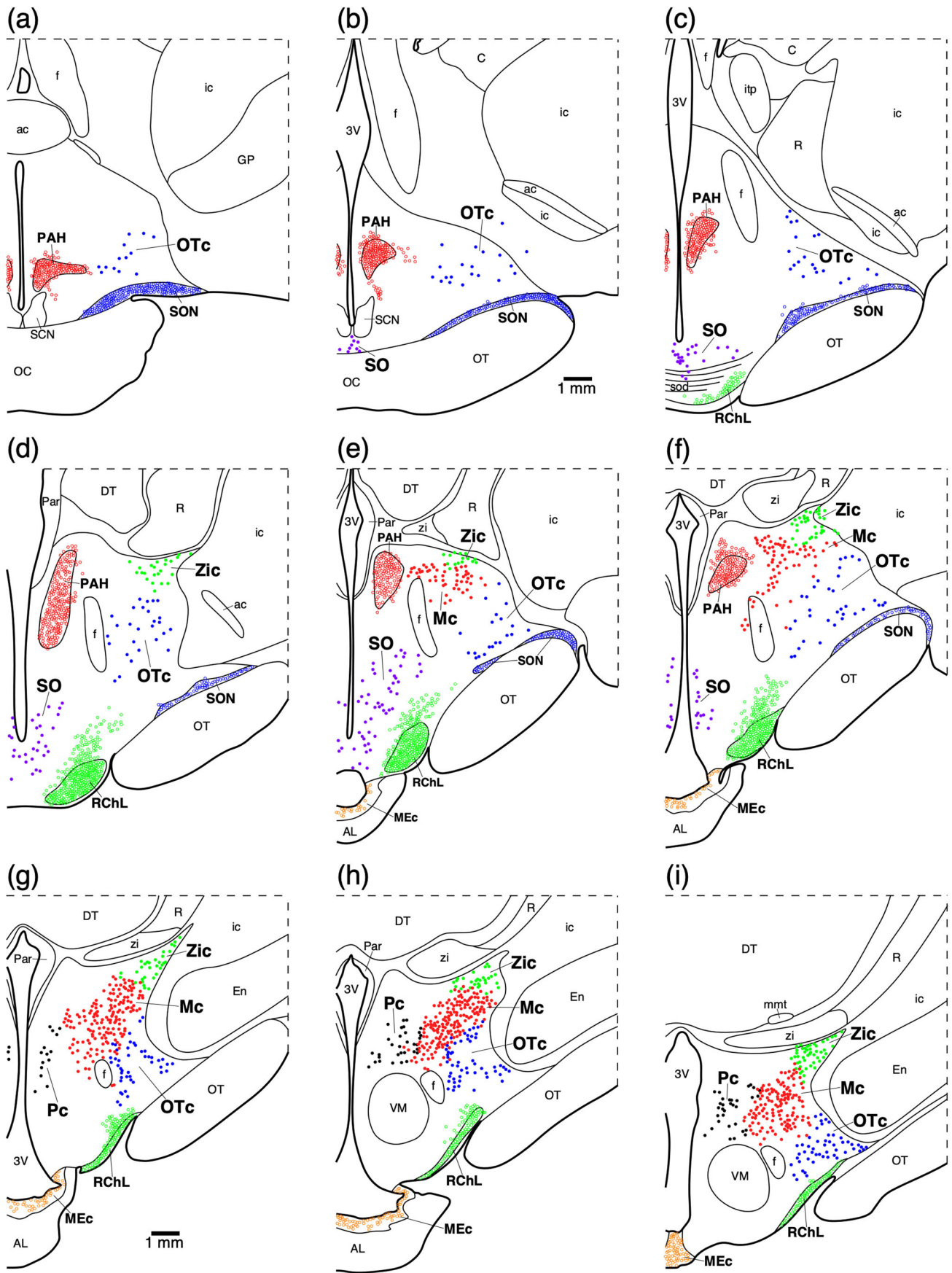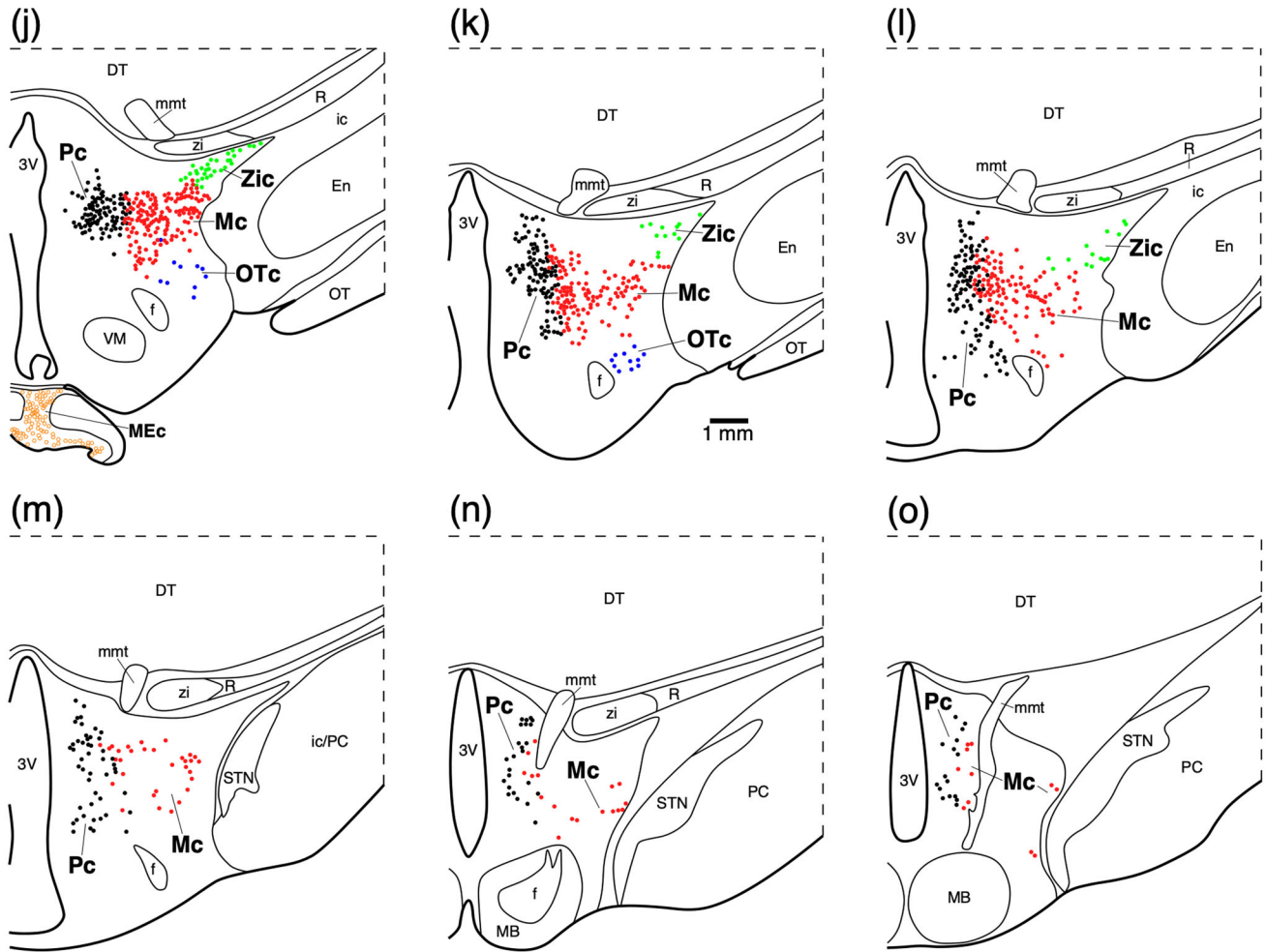
FIGURE 1

FIGURE 1 Continued

Serial drawings of coronal sections through one half of the Asiatic lion (*Panthera leo* subsp. *persica*) hypothalamus from the level of the decussation of the anterior commissure (ac) through to the mammillary bodies (MB) showing the distribution of orexin-A-immunopositive neurons. Panel (a) is the most rostral section and panel (o) the most caudal. The outlines of the architectonic regions were drawn from Nissl-stained sections, with orexin-A immunoreactive neurons marked on these drawings. Solid red circles represent orexinergic neurons of the main cluster (Mc), solid green circles represent orexinergic neurons of the zona incerta cluster (Zic), solid blue circles represent orexinergic neurons of the optic tract cluster (OTc), and solid black circles represent orexinergic neurons of the medially located parvocellular cluster (Pc). Potential additional clusters of orexinergic neurons were observed in the supraoptic region (SO, represented by solid purple circles), the paraventricular hypothalamus nucleus (PAH, represented by open red circles), the supraoptic nucleus (SON, represented by open blue circles), the lateral part of the retrochiasmatic area (RChL, represented by open green circles), and the internal layer of the median eminence (MEc, represented by open orange circles). Each circle represents an individual neuron. The maps are approximately 500 μm apart, and in each map dorsal is to the top and medial to the left.

felid species, we also observed a supraoptic cluster and a parvocellular cluster, clusters that are not typically reported in mammals (Figures 1 and 2). In the two subspecies of lion, we also observed potentially orexin-A-immunopositive neurons in the paraventricular hypothalamic nucleus, supraoptic nucleus, the lateral part of the retrochiasmatic area, and the inner layer of the median eminence (Figure 1).

3.1 | Main, zona incerta, and optic tract clusters

In mammals, orexinergic neurons are typically parcellated into three distinct clusters, a main cluster that houses the majority of the orex-

inergic neurons in the perifornical region, a zona incerta cluster in the dorsolateral aspect of the hypothalamus, and an optic tract cluster in the ventrolateral aspect of the hypothalamus (see Section 1). In all three felids investigated, these three clusters of orexinergic neurons were readily observed (Figures 1–6). The main cluster comprised the majority of orexinergic neurons and was localized to the regions surrounding the passage of the fornix through the hypothalamus, particularly lateral to the fornix (Figures 1e–o, 2a–n, 3b,d, 4b,d, and 5a,b,e). Emerging from this main cluster, orexinergic neurons were observed in the dorsolateral aspect of the hypothalamus, and these were assigned to the zona incerta cluster (Figures 1d–l, 2d–j, 3b,c, 4b,c, and 5a,c,f). These cells were most evident in the portion of the hypothalamus
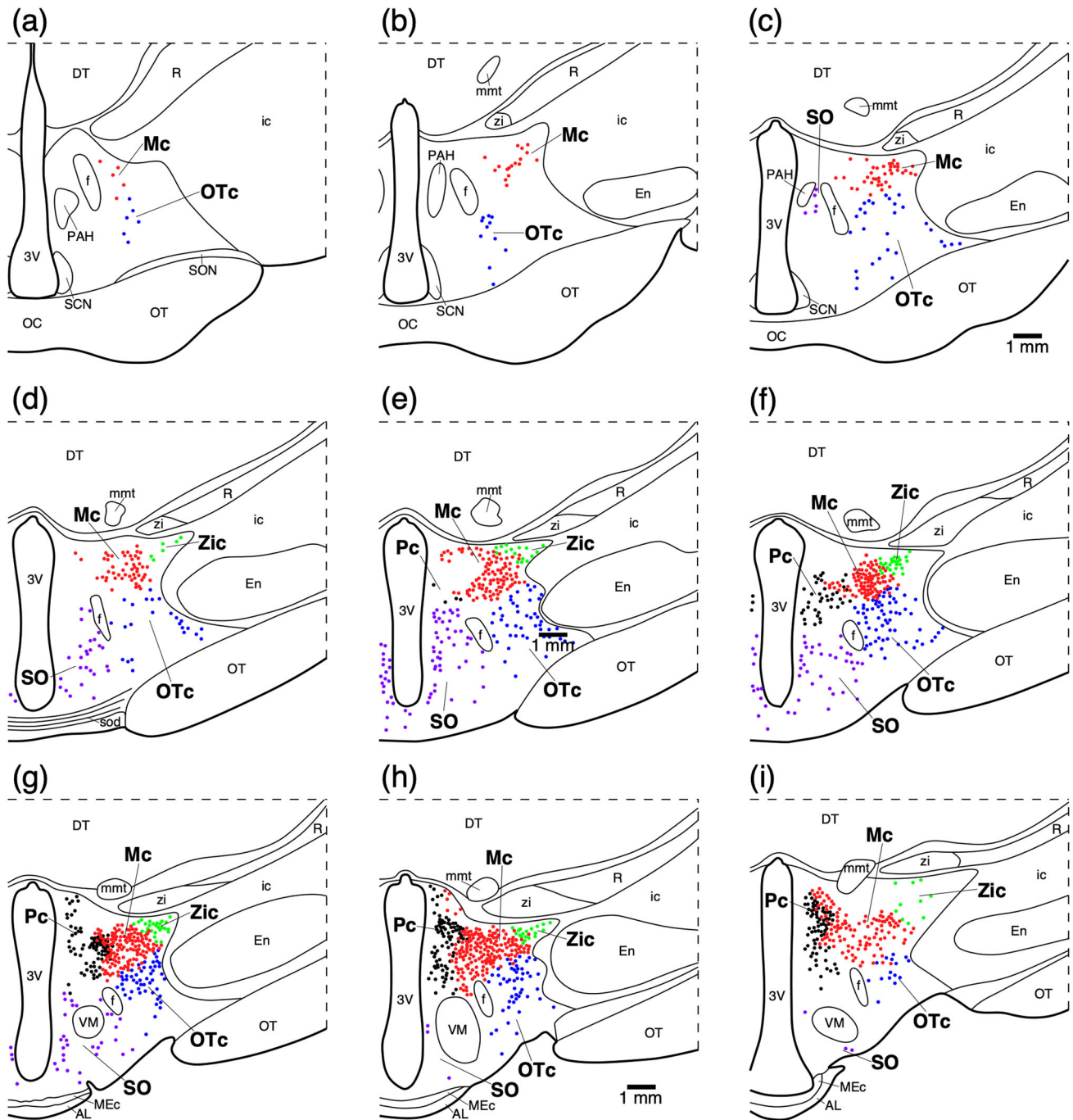
FIGURE 2

adjacent to the ventral border of the zona incerta. Emerging ventro-laterally from the main cluster, orexinergic neurons were observed in the ventrolateral hypothalamus dorsomedial to the optic tract, and these neurons were assigned to the optic tract cluster (Figures 1a–k, 2a–k, 3b,e, 4b,e, and 6b,c,e). The orexinergic neurons forming the main, zona incerta, and optic tract clusters were primarily bipolar in type, although multipolar neurons were evident (Figures 3–6). The neurons of the main cluster showed no distinct consistent dendritic orientation (Figures 3d, 4d, and 5b), but the dendrites of the zona incerta cluster neurons exhibited a distinct ventromedial–dorsolateral orientation

(Figures 3c, 4c, and 5c,f), while the dendrites of the neurons in the optic tract cluster exhibited a ventrolateral–dorsomedial orientation (Figures 3e, 4e, and 6e).

3.2 | Supraoptic cluster

Within the ventral half of the medial preoptic region (medial to the fornix), a low density of orexinergic neurons was observed in all three felids studied (Figures 1c–f, 2d–i, 6, and 7), which we term the

FIGURE 2 Continued

Serial drawings of coronal sections through one half of the Southeast African cheetah (*Acinonyx jubatus* subsp. *jubatus*) hypothalamus showing the distribution of orexin-A-immunopositive neu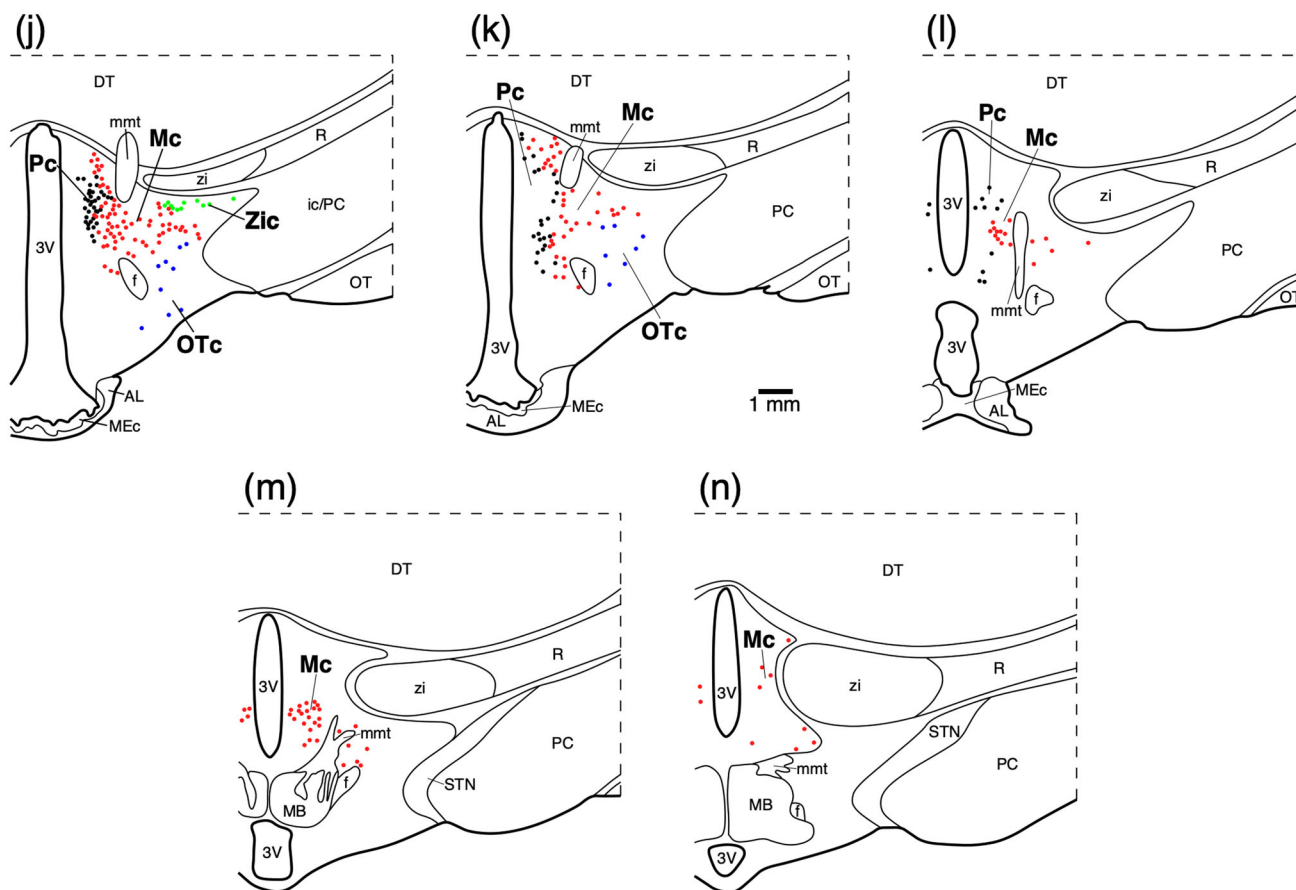rons. Panel (a) is the most rostral section and panel (n) the most caudal. The outlines of the architectonic regions were drawn using Nissl-stained sections and orexin-A immunoreactive neurons marked on these drawings. Solid red circles represent orexinergic neurons of the main cluster (Mc), solid green circles represent orexinergic neurons of the zona incerta cluster (Zic), solid blue circles represent orexinergic neurons of the optic tract cluster (OTc), solid black circles represent orexinergic neurons of the medially located parvocellular cluster (Pc), and solid purple circles represent the supraoptic cluster (SO). Each circle represents an individual neuron. The maps are approximately 500 μm apart, and in each map dorsal is to the top and medial to the left.

supraoptic orexinergic cluster. These supraoptic orexinergic neurons were located caudal to the suprachiasmatic nucleus and rostral to the ventromedial hypothalamic nucleus (Figures 1c-f and 2d-i). The supraoptic orexinergic neurons were primarily bipolar in type, although occasional multipolar neurons were present (Figures 6b,d,f, and 7). The passage of the fornix was used to distinguish between the supraoptic orexinergic cluster (medial to the fornix) and the optic tract cluster (lateral to the fornix in the lateral supraoptic region), as in most mammals no orexinergic neurons are observed in this region of the hypothalamus (although see Williams et al. [2022], where a similar distribution of orexinergic neurons was observed in the ventral half of the medial preoptic region in the lar gibbon and chimpanzee).

3.3 | Parvocellular cluster

Within the caudal half (caudal to the level of the ventromedial hypothalamic nucleus) of the medial zone of the hypothalamus, a moderately

densely packed cluster of orexinergic neurons that were significantly smaller in size than the other orexinergic neurons (see below) was observed in all three felids studied (Figures 1g–o, 2f–l, and 3–5). These neurons were assigned to the parvocellular orexinergic cluster, as they resemble similarly located orexinergic neurons observed in cetartiodactyls (Davimes et al., 2017; Dell et al., 2012; Dell, Karlsson, et al., 2016; Dell, Patzke, et al., 2016; Malungo et al., 2020) and the African elephant (Maseko et al., 2013). These parvocellular orexinergic neurons were distributed in a location medial to the main orexinergic cluster, with the smaller parvocellular neurons and larger main cluster neurons intermingling at their shared distributional limits, which aligns roughly with the passage of the fornix (Figures 1g–o, 2f–l, 3b,f, 4b,f, and 5a,d,g). The parvocellular orexinergic neurons approached but did not reach the lateral wall of the third ventricle. The majority of these parvocellular orexinergic neurons were bipolar, although occasional multipolar neurons were observed (Figures 3b,f, 4b,f, and 5a,d,g).

FIGURE 3 Low (a, b) and high (c–f) magnification photomicrographs of Nissl (a) and orexin-A-immunostained (b–f) sections through the hypothalamus (Hyp) of the Asiatic lion showing the neuronal morphology and location of four orexinergic neuronal clusters, the zona incerta cluster (Zic; b, c), the main cluster (Mc; b, d), the optic tract cluster (OTc; b, e), and the parvocellular cluster (Pc; b, f). Note the specific dendritic orientations of these neurons in the Zic (c) and OTc (e) as compared to the lack of a specific orientation in the Mc (d). Also, note the smaller size of the soma in the Pc (f) compared to the other clusters. In all images, dorsal is to the top and medial to the left. Scale bar in panel (b) = 500 μm and applies to panels (a) and (b). Scale bar in (f) = 50 μm and applies to (c–f).
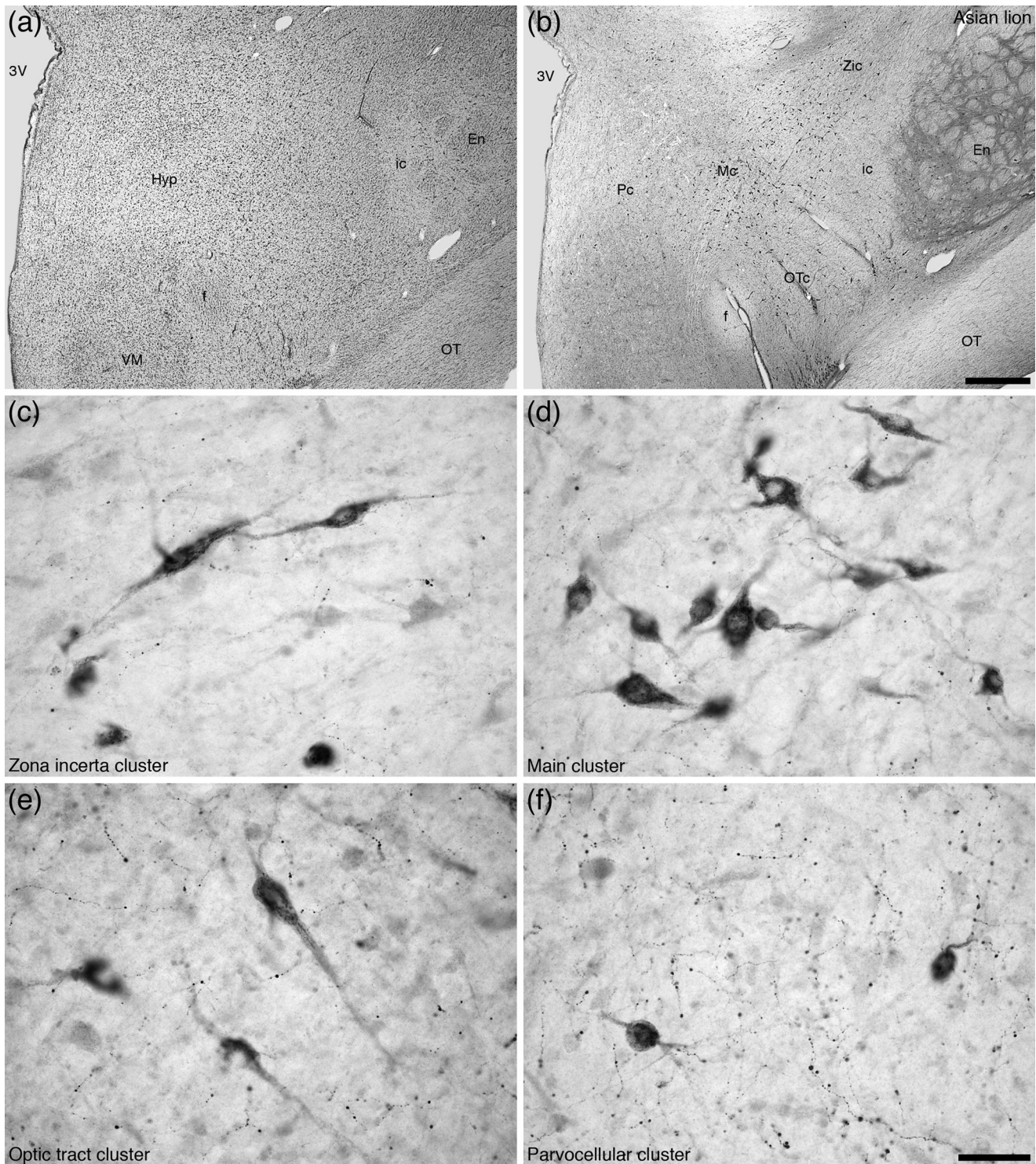
FIGURE 4 Low (a, b) and high (c–f) magnification photomicrographs of Nissl (a) and orexin-A-immunostained (b–f) sections through the hypothalamus (Hyp) of the African lion showing the neuronal morphology and location of four orexinergic neuronal clusters, the zona incerta cluster (Zic; b, c), the main cluster (Mc; b, d), the optic tract cluster (OTc; b, e), and the parvocellular cluster (Pc; b, f). Note the specific dendritic orientations of these neurons in the Zic (c) and OTc (e) as compared to the lack of a specific orientation in the Mc (d). Also, note the smaller size of the soma in the Pc (f) compared to the other clusters. In all images, dorsal is to the top and medial to the left. Scale bar in panel (b) = 500 μm and applies to panels (a) and (b). Scale bar in (f) = 50 μm and applies to panels (c–f).
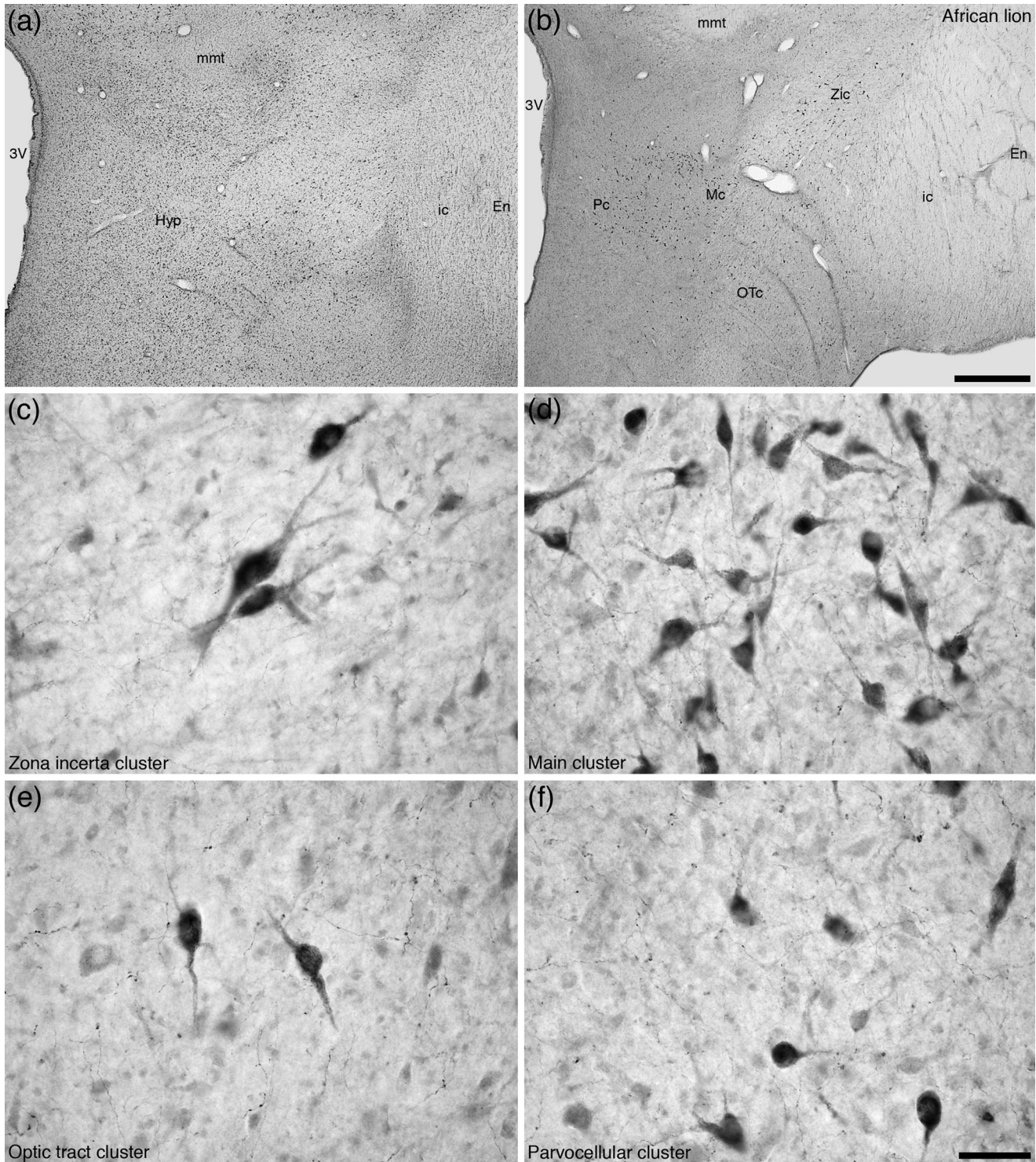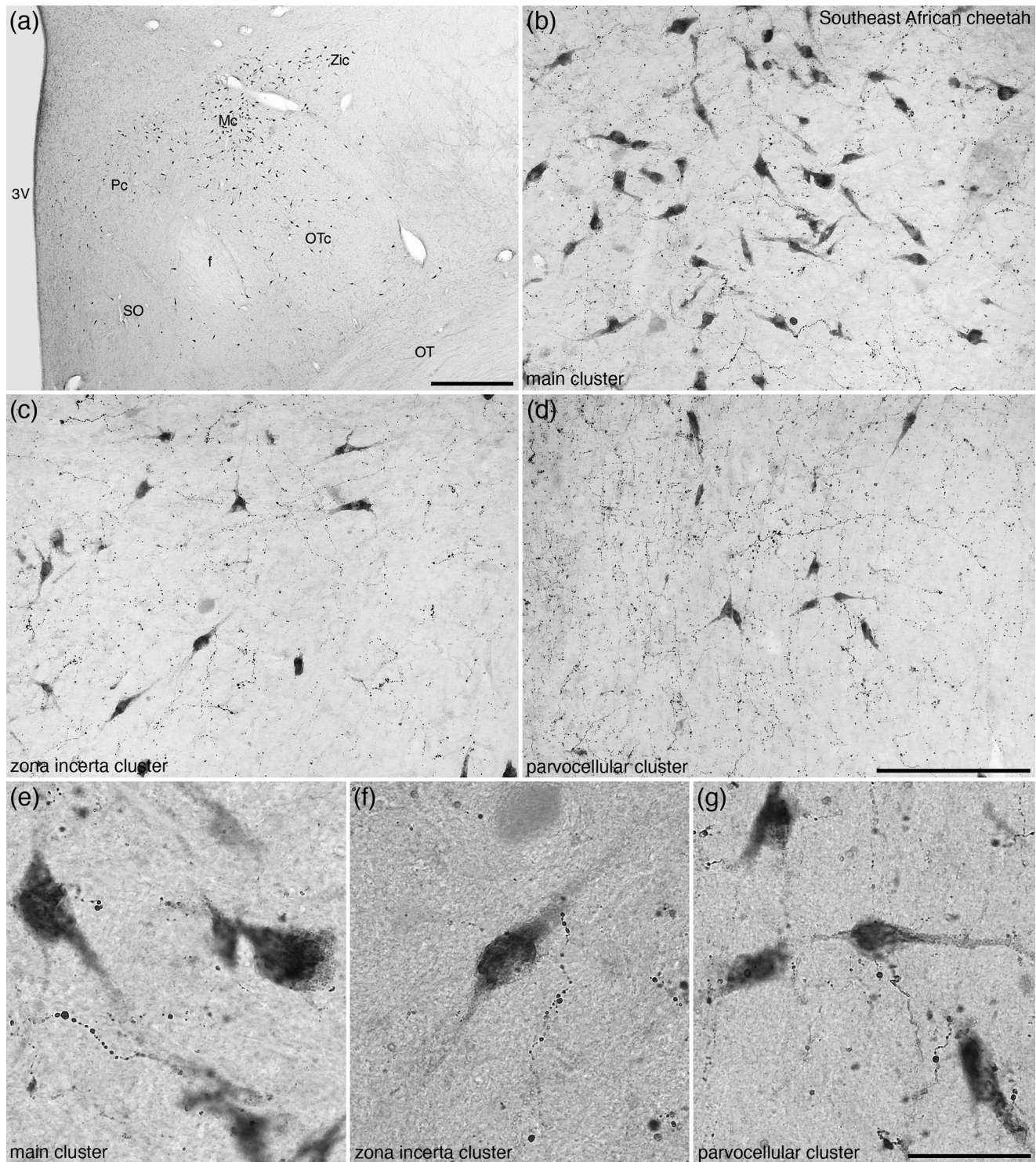
FIGURE 5 Low (a) and higher (b–g) magnification photomicrographs of orexin-A-immunostained sections through the hypothalamus of the Southeast African cheetah showing the location and neuronal morphology of the orexinergic neuronal clusters observed. (a) In the hypothalamus of the cheetah, we observed the main cluster (Mc), the zona incerta cluster (Zic), the optic tract cluster (OT), the supraoptic cluster (SO), and the parvocellular cluster (Pc). (b–g) The majority of these orexinergic neurons were bipolar, but there were also several multipolar neurons. Also, note the smaller size of the soma in the Pc (g) compared to the other clusters. In all images, dorsal is to the top and medial to the left. Scale bar in panel (a) = 1 mm and applies to panel (a) only. Scale bar in panel (d) = 250 μm and applies to panels (b), (c), and (d). Scale bar in panel (g) = 50 μm and applies to panels (e), (f), and (g).

ODDES ET AL.
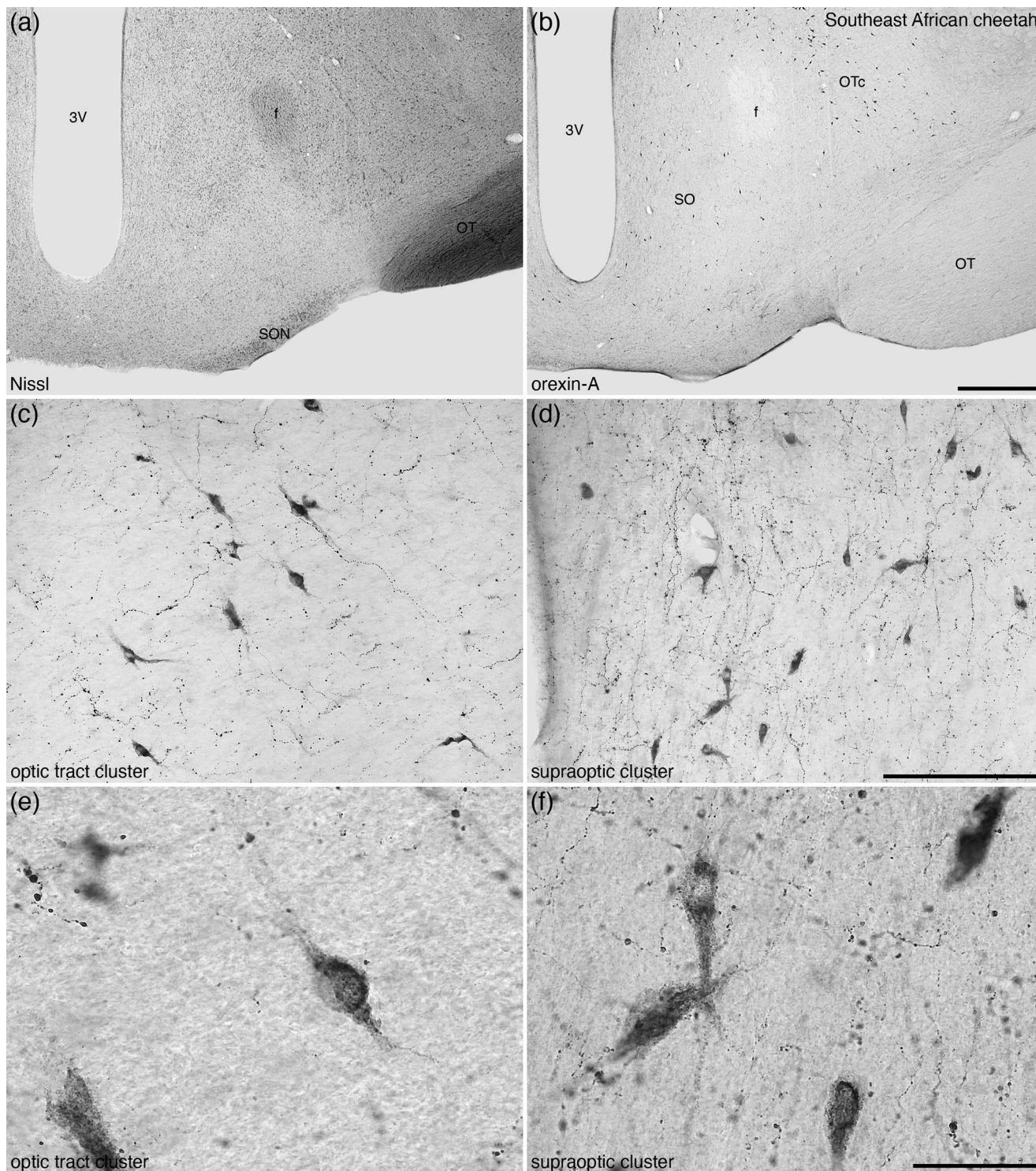
FIGURE 6 Photomicrographs at different magnifications of Nissl (a) orexin-A-immunostained (b–f) coronal sections through the medial supraoptic region of the Southeast African cheetah hypothalamus. What appears to be intensely orexin-A immunoreactive bipolar neurons are evident in this region, forming the supraoptic orexinergic cluster (SO). Note that the SO cluster is distinguished from the optic tract cluster (OTc) by the passage of the fornix (f). (f) The neurons forming the OTc are also bipolar. In all images, dorsal is to the top and medial to the left. Scale bar in panel (b) = 1 mm and applies to panels (a) and (b). Scale bar in panel (d) = 250 μm and applies to panels (c) and (d). Scale bar in panel (f) = 50 μm and applies to panels (e) and (f).
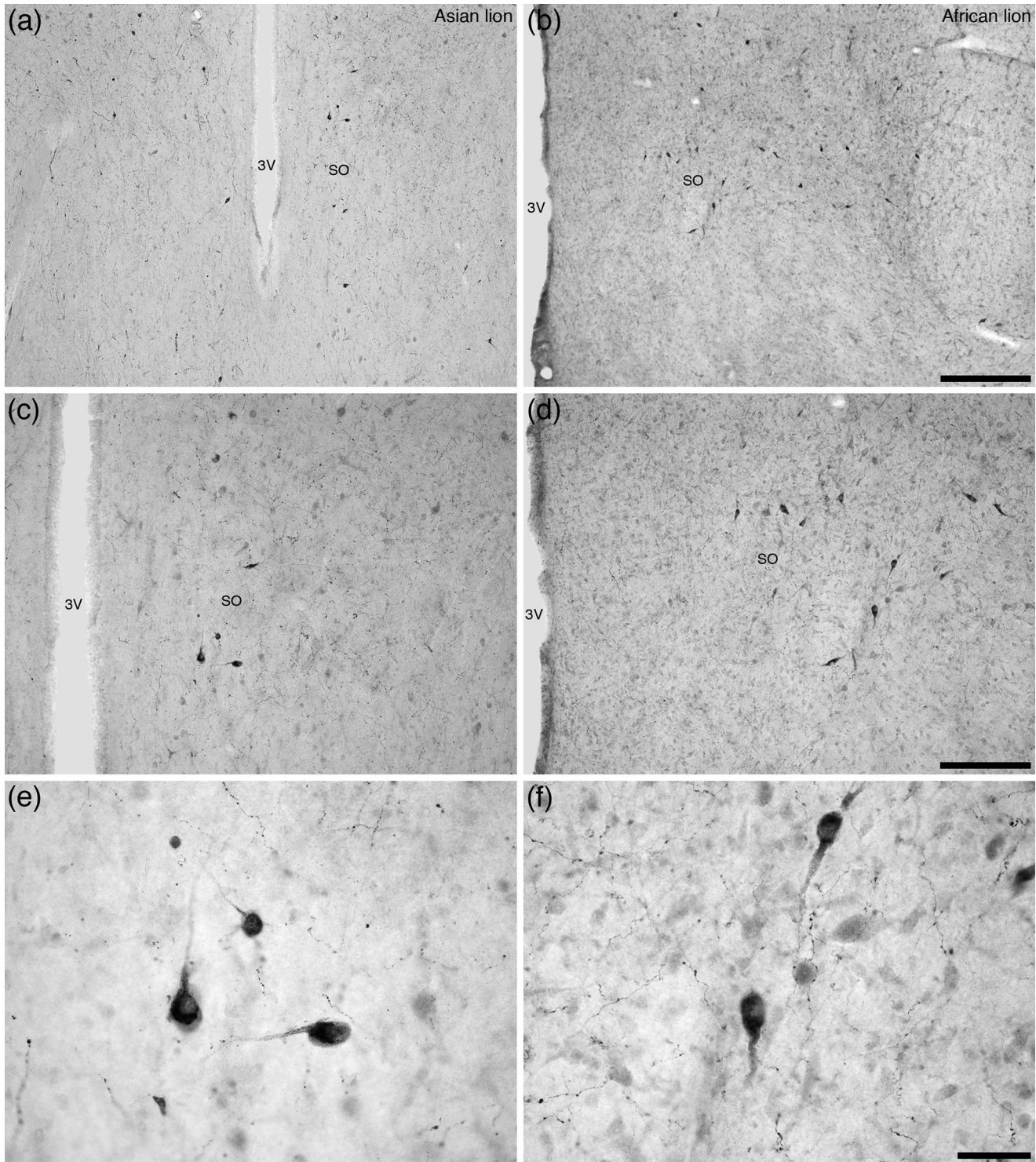
FIGURE 7 Photomicrographs at different magnifications of orexin-A-immunostained coronal sections through the medial supraoptic region of the Asiatic (a, c, e) and African (b, d, f) lion. What appears to be intensely orexin-A immunoreactive bipolar neurons are evident in this region in both subspecies, forming the supraoptic orexinergic cluster (SO). In all images, dorsal is to the top and medial to the left. Scale bar in panel (b) = 500 µm and applies to panels (a) and (b). Scale bar in panel (d) = 250 µm and applies to panels (c) and (d). Scale bar in panel (f) = 50 µm and applies to panels (e) and (f).

**TABLE 1** Stereological parameters used for estimating the number of neurons immunopositive for orexin-A in the felids studied

Species	Nucleus examined	Counting frame size (µm)	Sampling grid size (µm)	Dissector height (µm)	Cut thickness (µm)	Average mounted thickness (µm)	Vertical guard zones (top and bottom, µm)	Section interval	Number of sections	Number of sampling sites	Average CE (Gundersen m = 0)	Average CE (Gundersen m = 1)
Asiatic lion	Other (OTc, SO, Zic, Mc)	150 × 150	350 × 350	17	50	23.4	4	10	16	247	0.07	0.05
	PC	150 × 150	350 × 350	17	50	23.4	4	10	16	247	0.09	0.08
African lion	Other (OTc, SO, Zic, Mc)	150 × 150	450 × 450	15	50	24.4	4	10	12	139	0.08	0.07
	PC	150 × 150	450 × 450	15	50	24.4	4	10	12	139	0.18	0.13
Southeast African cheetah	Other (OTc, SO, Zic, Mc)	150 × 150	450 × 450	15	50	22.4	4	10	14	244	0.12	0.07
	PC	150 × 150	450 × 450	15	50	22.4	4	10	14	244	0.15	0.12

Abbreviations: Mc, main orexinergic cluster; OTc, optic tract orexinergic cluster; PC, parvocellular orexinergic cluster; SO, supraoptic orexinergic cluster; Zic, zona incerta orexinergic cluster.

3.4 | Stereological analyses of main, zona incerta, optic tract, supraoptic, and parvocellular clusters

As indicated above, the neuronal morphology of the orexinergic neurons in the main, zona incerta, optic tract, and supraoptic clusters was very similar. Due to this, and their topographical continuity within the hypothalamus, quantitative neuronal parameters regarding these four clusters have been grouped. In contrast, due to the clearly smaller size of the orexinergic neurons in the parvocellular cluster, these have been analyzed separately (Tables 1 and 2). For the four clusters in the Asiatic lion, the stereologically estimated total orexinergic neuronal population was 70,634. In the African lion, the estimated population was 68,474, while in the Southeast African cheetah the estimated population was 65,530. The average soma volume for these four clusters was 3307.35 µm^3 in the Asiatic lion, 4299.26 µm^3 in the African lion, and 4391.17 µm^3 in the Southeast African cheetah. The average soma area for these four clusters was 238.86 µm^2 in the Asiatic lion, 288.61 µm^2 in the African lion, and 295.92 µm^2 in the Southeast African cheetah. It is interesting to note that the Asiatic lion, with a brain mass of 184.4 g, had the highest estimated neuronal population, while the Southeast African cheetah, with the smallest brain mass of the species investigated (139.8 g), had the lowest neuronal population estimate. In contrast, the Southeast African cheetah presented with the largest soma volumes and areas, while the Asiatic lion had the smallest volumes and areas (Table 2). The quantitative data for the African lion, with a brain mass of 166.4 g, which lies between that of the two other species, had population estimates and soma volumes and areas that also were intermediate between the two other felids studied.

The estimated parvocellular orexinergic neuronal population in the Asiatic lion was 28,252, in the African lion 19,312, and in the Southeast African cheetah 18,260 (Table 2). In terms of soma volume, the average observed for the Asiatic lion was 1514.67 µm^3, for the African lion 1618.26 µm^3, and 1014.21 µm^3 for the Southeast African cheetah (Table 2). For soma area in the parvocellular cluster, the average observed for the Asiatic lion was 142.15 µm^2, for the African lion 143.55 µm^2, and for the Southeast African cheetah 112.49 µm^2 (Table 2). Thus, while the estimated population appears to roughly correlate with brain mass (the larger brained Felids having more neurons), the African lion presented with the largest soma volumes and areas, and the Southeast African cheetah the smallest (Table 2), thus not following the pattern observed for the larger orexinergic neurons in the four clusters noted above.

3.5 | Potential additional clusters in the Asiatic and African lions

Within the two subspecies of lion, substantial neuronal populations within the paraventricular hypothalamic nucleus, supraoptic nucleus, and the lateral part of the retrochiasmatic area (Figures 1a-i and 8–10) appeared to be orexin-A-immunopositive. These potentially orexinergic neuronal populations were not observed in the brain of the Southeast African cheetah. Unlike the intensity of the

FIGURE 8 Photomicrographs of Nissl stained (a) and orexin-A-immunostained (b–f) coronal sections through the paraventricular hypothalamic nucleus (PAH) of the Asiatic (a–d) and African (e, f) lion. What appears to be moderately intensely immunoreactive neurons are evident throughout this nucleus in both subspecies, with scattered neurons surrounding the architectonically distinct portion of this nucleus. Note the presence of intensely orexin-A immunoreactive boutons that are distinct from these PAH neurons. The presence of these axons indicates that the cellular staining in this region may be a false-positive staining. In all images, dorsal is to the top and medial to the left. Scale bar in panel (b) = 500 μm and applies to panels (a) and (b). Scale bar in panel (e) = 250 μm and applies to panels (c) and (e). Scale bar in panel (f) = 50 μm and applies to panels (d) and (f).

TABLE 2 Stereological results for cell numbers, volume, and area in the Asiatic lion, African lion, and Southeast African cheetah

Species	Nucleus examined	Brain mass (g)	Total estimated population using mean section thickness	Average estimated cell volume (μm^3)	Average estimated cell area (μm^2)
Asiatic lion	PC	184.4	28 252	1514.67	142.15
	Other (OTc, SO, Zic, Mc)		70 634	3307.35	238.86
African lion	PC	166.4	19 312	1618.26	143.55
	Other (OTc, SO, Zic, Mc)		68 474	4299.26	288.61
Southeast African cheetah	PC	139.8	18 260	1014.21	112.49
	Other (OTc, SO, Zic, Mc)		65 530	4391.17	295.92

Abbreviations: Mc, main orexinergic cluster; OTc, optic tract orexinergic cluster; PC, parvocellular orexinergic cluster; SO, supraoptic orexinergic cluster; Zic, zona incerta orexinergic cluster.

immunoreactivity observed within the neurons forming the clusters described above, within these three hypothalamic locations the staining intensity was appreciably lighter, often with nuclei visible at the center of the soma (Figures 8–10). In all three locations, the vast majority of neurons within each location displayed this type of staining (Figures 8–10). Despite the less intense immunoreactivity and high proportion of neurons immunostained, these locations were very specific, and the distribution of the immunostained neurons was not generalized but localized to the distinct nuclei/parts and did not extend into adjacent regions (Figures 8a,b, 9a,b, and 10a,b).

Orexin-A-immunoreactive structures were also observed in the inner layer of the median eminence (Figures 1e-j and 11). What appears to be faintly immunoreactive tanycytes were evident within the internal layer of the median eminence, as well as intensely immunoreactive smaller cells that appear to be macrophages (Figure 11). No distinct orexin-A immunostaining was observed in the external layer of the median eminence or in the vessels comprising the anterior lobe of the pituitary gland (Figure 11).

4 | DISCUSSION

The current study employed immunohistochemical staining with an orexin-A antibody to reveal orexinergic neurons within the hypothalami of three felids—an Asiatic lion, an African lion, and a Southeast African cheetah—extending previous observations in the domestic cat, which is also a species belonging to the Felidae but phylogenetically distinct to the other carnivores (domestic dog, domestic ferret, and banded mongoose) previously studied (Bininda-Emonds, Gittleman, & Purvis, 1999). As observed across many mammals studied to date (see Table 3 and references therein), the orexinergic neurons were limited in their distribution to the hypothalamus with only rare orexinergic neurons located immediately adjacent to the hypothalamus. Within the hypothalami of the three felids studied, several clusters of orexinergic neurons were observed. These cluster include the main, zona incerta, and optic tract clusters that are typically observed across mam-

mals (Table 3 and references cited therein), although it should be noted that the precise delineation of these clusters, while based on neuronal morphology, may have some errors. In addition to these three typically identified orexinergic neuronal clusters, we observed orexinergic neurons in the ventromedial supraoptic region that we term the supraoptic orexinergic cluster, as well as a medially located cluster of orexinergic neurons with substantially smaller soma volumes that we term the parvocellular cluster. In the Asiatic and African lions, but not in the Southeast African cheetah, we observed immunopositivity to the orexin-A antibody used in the neurons of the paraventricular hypothalamic nucleus, supraoptic nucleus, and the lateral part of the retrochiasmatic area, as well as potential tanycytes and macrophages in the inner layer of the median eminence, nuclei/regions that rarely exhibit immunopositivity to orexin antibodies. These findings are discussed in a phylogenetic and functional context.

4.1 | Main, zona incerta, and optic tract orexinergic clusters

Across the mammalian species in which the distribution and parcellation of orexinergic neurons have been defined (Table 3), the most often identified clusters of orexinergic neurons are the main, zona incerta, and optic tract clusters (Nixon & Smale, 2007). In the three felids studied herein, these three orexinergic clusters were readily identified. The only exception noted to date regarding these three orexinergic clusters is the lack of the optic tract cluster in microchiropteran bats (Kruger et al., 2010). Thus, the main, zona incerta, and optic tract orexinergic clusters appear to form the primary neuronal basis of the orexinergic system in mammals. It would appear reasonable to conclude, due to the lack of phylogenetic variance regarding these three orexinergic clusters, that the functions associated with the orexinergic neurons forming these clusters (e.g., Inutsuka & Yamanaka, 2013; Kukkonen et al., 2002; Soya & Sakurai, 2020; Zhang et al., 2013) are likely to be consistent across mammalian species, including the three felid species studied herein.

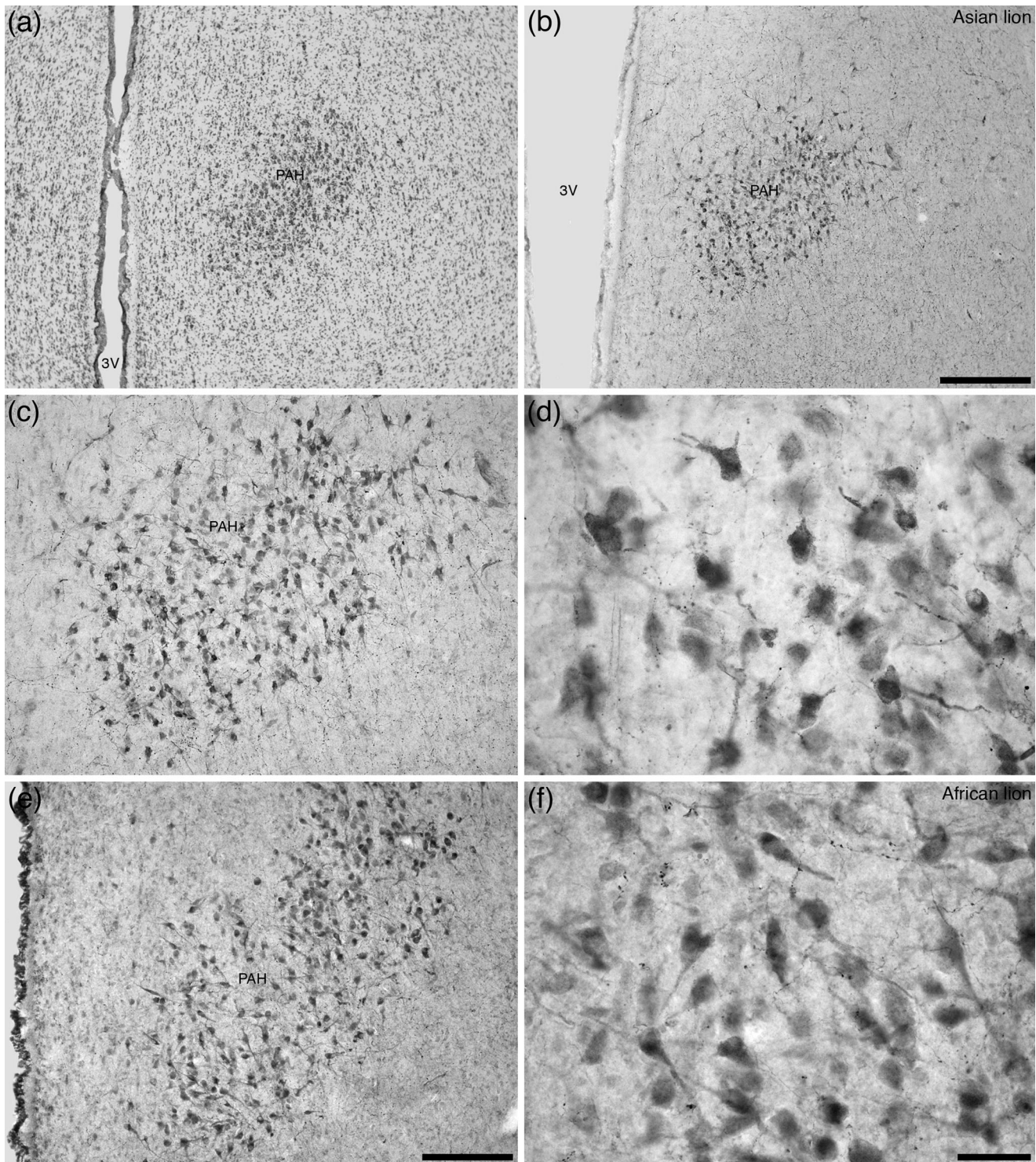**FIGURE 9** Photomicrographs of Nissl stained (a) and orexin-A-immunostained (b–f) coronal sections through the supraoptic nucleus (SON) of the Asiatic (a–d) and African (e, f) lion. What appears to be moderately intensely immunoreactive neurons are evident throughout this nucleus in both subspecies. In all images, dorsal is to the top and medial to the left. Scale bar in panel (b) = 500 μm and applies to panels (a) and (b). Scale bar in panel (e) = 250 μm and applies to panels (c) and (e). Scale bar in panel (f) = 50 μm and applies to panels (d) and (f).

4.2 | Supraoptic orexinergic cluster

In the current study, we identified a low-density cluster of orexin-A-immunopositive neurons with large soma in the medial supraoptic region of the three felids studied, which we term the supraoptic orex- inergic cluster. In previous studies of carnivores (Table 3; Pillay et al., 2017; Thannickal et al., 2000; Wagner et al., 2000; Zhang et al., 2001) and the closely related pangolin (Imam et al., 2019), orexinergic neu- rons were not observed in this region of the hypothalamus. Indeed, across most mammals that have been investigated, orexinergic neurons
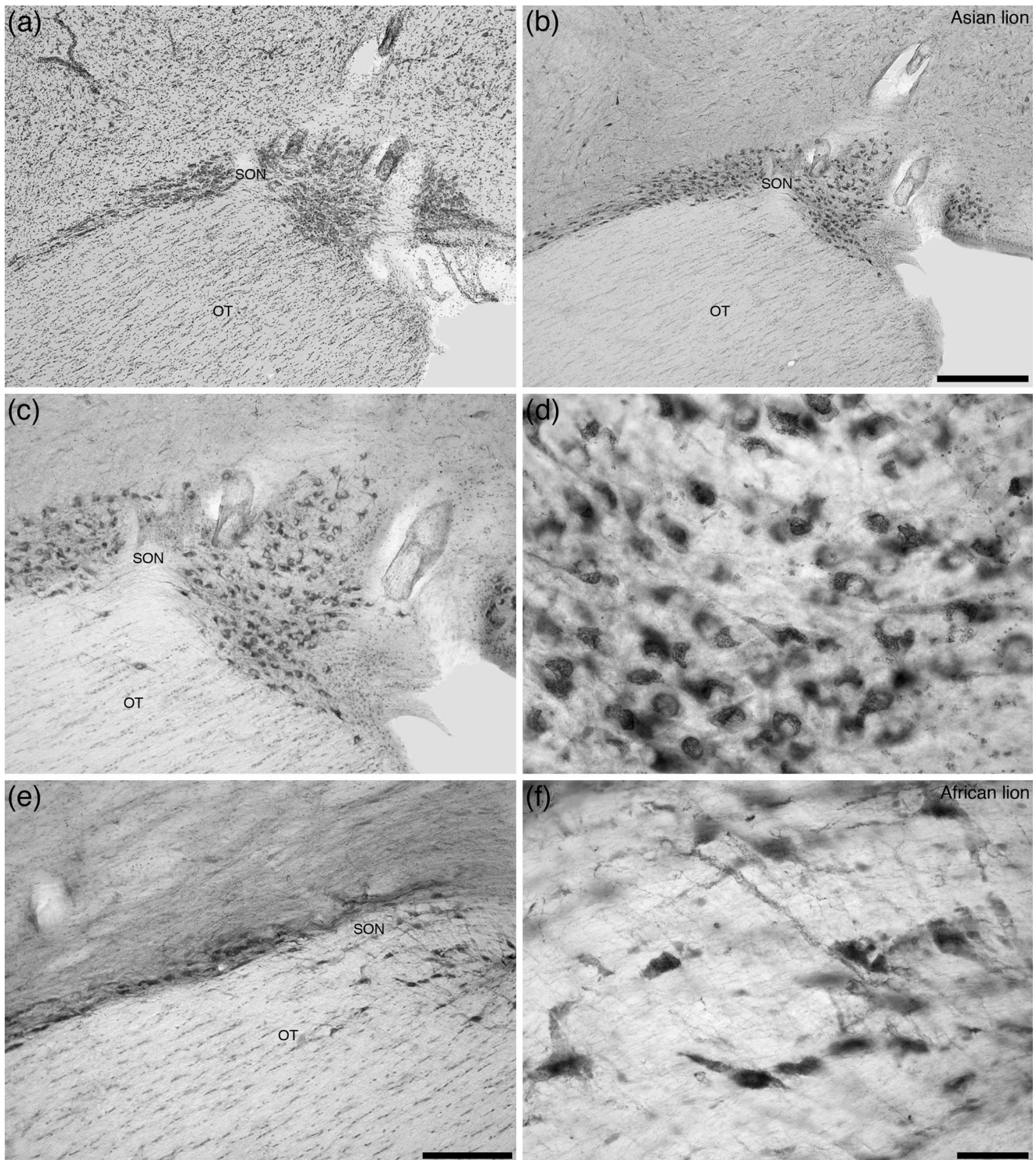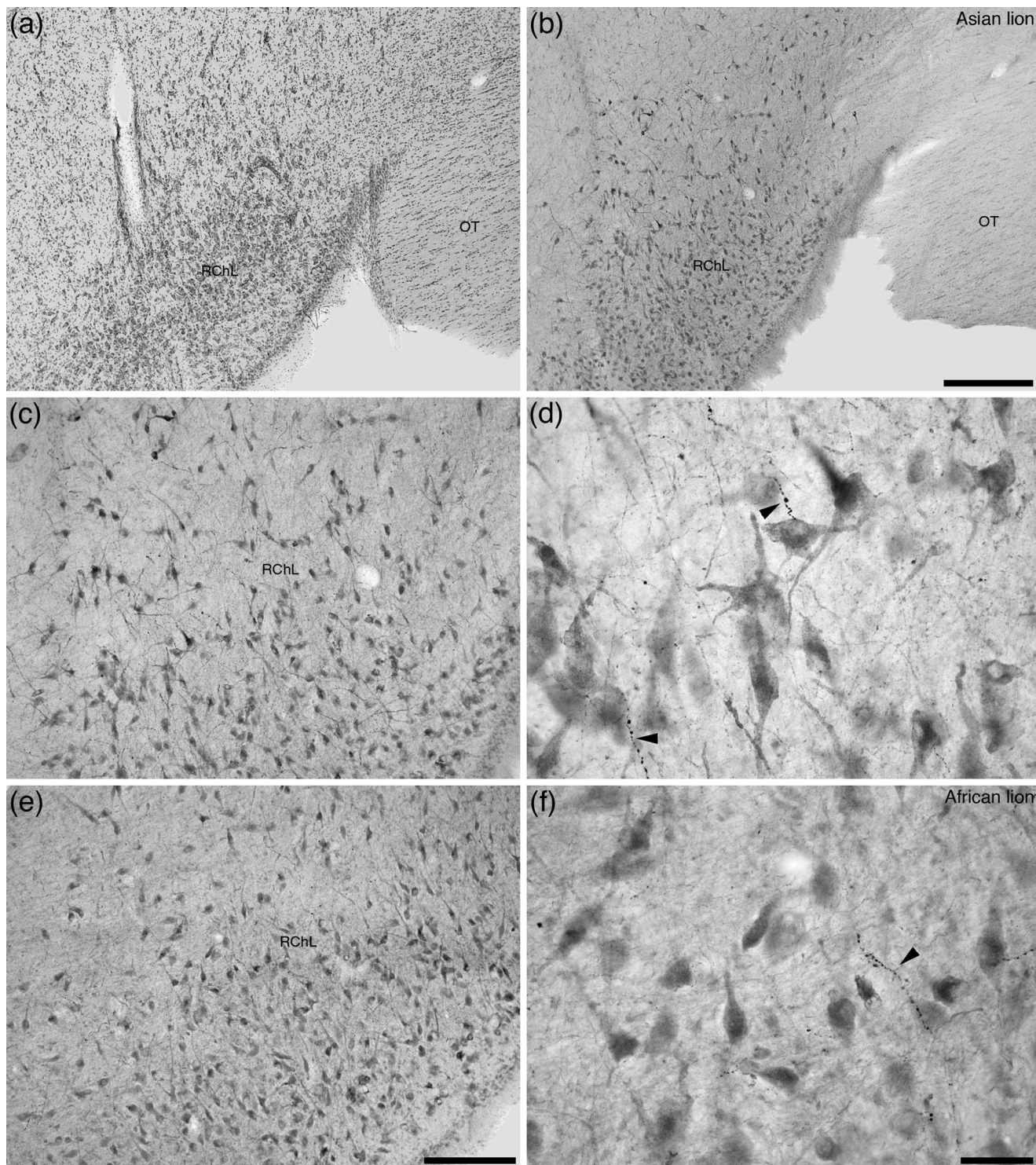
FIGURE 10 Photomicrographs of Nissl stained (a) and orexin-A-immunostained (b–f) coronal sections through the retrochiasmatic area, lateral part (RChL) of the Asiatic (a–d) and African (e, f) lion. What appears to be moderately intensely immunoreactive neurons are evident throughout this nucleus in both subspecies, with scattered neurons extending dorsally. Note the presence of intensely orexin-A immunoreactive boutons (arrowheads in panels d and f) that are distinct from these neurons. The presence of these axons indicates that the cellular staining in this region may be a false-positive staining. In all images, dorsal is to the top and medial to the left. Scale bar in panel (b) = 500 μm and applies to panels (a) and (b). Scale bar in panel (e) = 250 μm and applies to panels (c) and (e). Scale bar in panel (f) = 50 μm and applies to panels (d) and (f).
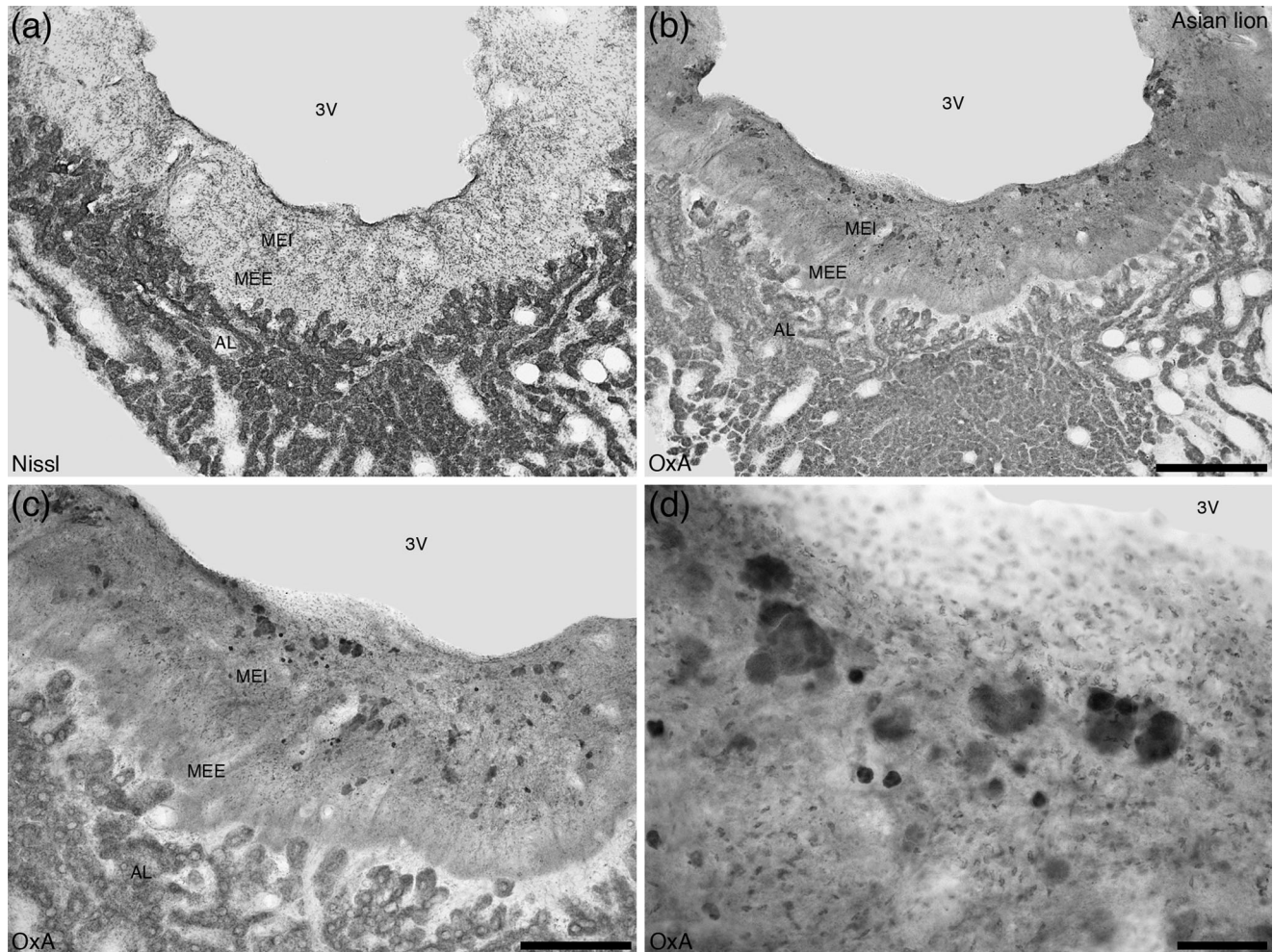
FIGURE 11 Photomicrographs of Nissl stained (a) and orexin-A-immunostained (b–d) coronal sections through the median eminence of the Asiatic lion. What appears to be palely immunoreactive tanycytes are evident within the internal layer of the median eminence (MEI), as well as intensely immunoreactive smaller cells that appear to be macrophages. No distinct orexin-A immunostaining is observed in the external layer of the median eminence (MEE) or in the vessels comprising the anterior lobe of the pituitary gland (AL). In all images, dorsal is to the top. Scale bar in panel (b) = 500 μm and applies to panels (a) and (b). Scale bar in panel (c) = 250 μm. Scale bar in panel (d) = 50 μm

have not been reported in this region of the hypothalamus (Table 3). The one exception is the report of similar orexinergic neurons being observed in the ventromedial supraoptic region of the lar gibbon and chimpanzee (Williams et al., 2022). In the lar gibbon and chimpanzee, these ventromedial supraoptic orexinergic neurons were described as a medial extension of the optic tract cluster, as they were few in number (Williams et al., 2022). In the current study, while the numbers of neurons and their packing density was low in comparison to the main, zona incerta, and optic tract clusters, their relative number and density was greater than seen in the lar gibbon and chimpanzee (Williams et al., 2022). For this reason, in the current study we have defined these orexinergic neurons that are found medial to the passage of the fornix, as a distinct supraoptic orexinergic cluster. In addition, the morphology of these supraoptic orexinergic neurons, particular the volume of the soma, was similar to that observed in the main, zona incerta, and optic tract clusters. Thus, these medial supraoptic orexinergic neurons appear to be what we could term additional "typical" orexinergic neurons, based on soma size and dendritic morphology.

The neurons of the medial supraoptic region of the hypothalamus are involved in many different functions, including the control of blood pressure, water balance, thermoregulation, eating, reproduction, daily rhythms, stress and metabolic control, and sleep and arousal (e.g., Pop, Crivii, & Opincariu, 2018); however, it is difficult to postulate the precise role the activity of these sparsely distributed orexinergic neurons may play in these functions. Despite this, the noting of their presence is of importance, as they are also found in the apes that have been studied, and may be present in humans (Williams et al., 2022). The presence of the supraoptic orexinergic cluster in the felids studied, in some apes, and potentially also in humans indicates one possible avenue for increasing the organizational and associated functional complexity of the orexinergic system in mammals.

4.3 | Parvocellular orexinergic cluster

An additional, atypical cluster of orexinergic neurons observed in the brains of the three felids studied was the parvocellular orexinergic

TABLE 3 Summary of reported orexinergic neuronal populations (or clusters) in the hypothalamus of 54 mammal species/subspecies/strains

Clade/Order/*Genus species*	Common name	Orexinergic neuronal populations/clusters									Source
		Mc	Zic	OTc	SO	Pc	PAH	SON	RChL	ME	
Metatheria											
Diprotodontia											
Macropus giganteus	Eastern gray kangaroo	✓	✓	✓	×	×	×	×	×	×	1
Dasyuromorphia											
Sarcophilus harrisii	Tasmanian devil	✓	✓	✓	×	×	×	×	×	×	2
Eutheria											
Pholidota											
Manis tricuspis	Tree pangolin	✓	✓	✓	×	×	×	×	×	×	3
Carnivora											
Mustela putorius subsp. *furo*	Domestic ferret	✓	✓	✓	×	×	×	×	×	×	4
Canis lupus subsp. *familiaris*	Domestic dog	✓	✓	✓	×	×	×	×	×	×	5
Mungos mungo	Banded mongoose	✓	✓	✓	×	×	×	×	×	×	4
Felis catus	Domestic cat	✓	✓	✓	×	×	×	×	×	×	6
Panthera leo subsp. *leo*	Asiatic lion	✓	✓	✓	✓	✓	✓	✓	✓	✓	7
Panthera leo subsp. *melanochaita*	African lion	✓	✓	✓	✓	✓	✓	✓	✓	✓	7
Acinonyx jubatus subsp. *jubatus*	Southeast African cheetah	✓	✓	✓	✓	✓	×	×	×	×	7
Chiroptera											
Cardioderma cor	Heart-nosed bat	✓	✓	×	×	×	×	×	×	×	8
Chaerephon pumilus	Little free-tailed bat	✓	✓	×	×	×	×	×	×	×	8
Coleura afra	African sheath-tailed bat	✓	✓	×	×	×	×	×	×	×	8
Hipposideros commersoni	Commerson's roundleaf bat	✓	✓	×	×	×	×	×	×	×	8
Triaenops persicus	Persian trident bat	✓	✓	×	×	×	×	×	×	×	8
Eidolon helvum	Straw-colored fruit bat	✓	✓	✓	×	×	×	×	×	×	9
Epomophorus wahlbergi	Wahlberg's epauletted fruit bat	✓	✓	✓	×	×	×	×	×	×	9
Soricidae											
Crocidura cyanea	Reddish-gray musk shrew	✓	✓	✓	×	×	×	×	×	×	10
Crocidura olivieri	African giant shrew	✓	✓	✓	×	×	×	×	×	×	10
Sylvisorex ollula	Greater forest shrew	✓	✓	✓	×	×	×	×	×	×	10
Erinaceidae											
Paraechinus aethiopicus	Desert hedgehog	✓	✓	✓	×	×	×	×	×	×	10
Atelerix frontalis	Southern African hedgehog	✓	✓	✓	×	×	×	×	×	×	10
Cetartiodactyla											
Giraffa camelopardalis	Giraffe	✓	✓	✓	×	✓	×	×	×	×	11

(Continues)

TABLE 3 (Continued)

Clade/Order/*Genus species*	Common name	Orexinergic neuronal populations/clusters									Source
		Mc	Zic	OTc	SO	Pc	PAH	SON	RChL	ME	
Oryx leucoryx	Arabian oryx	✓	✓	✓	×	✓	×	×	×	×	12
Connochaetes taurinus	Blue wildebeest	✓	✓	✓	×	✓	×	×	×	×	13
Ovis aries	Domestic sheep	✓	✓	✓	×	✓	×	×	×	×	14
Hippopotamus amphibius	River hippopotamus	✓	✓	✓	×	✓	×	×	×	×	15
Phocoena phocoena	Harbor porpoise	✓	✓	✓	×	✓	×	×	×	×	11
Balaenoptera acutorostrata	Minke whale	✓	✓	✓	×	✓	×	×	×	×	16
Sus scrofa domesticus	Göttingen minipig	✓	✓	✓	×	✓	×	×	×	×	17
Rodentia											
Rattus norvegicus	Laboratory rat, Long–Evans strain	✓	✓	✓	×	×	✓	✓	×	×	18
Rattus norvegicus	Laboratory rat, Sprague–Dawley strain	✓	✓	✓	×	×	×	×	×	✓	19
Mus minutoides	African pygmy mouse	✓	✓	✓	×	×	×	×	×	×	20
Mesocricetus auratus	Golden/Syrian hamster	✓	✓	✓	×	×	✓	✓	×	×	18
Arvicanthis niloticus	Nile grass rat	✓	✓	✓	×	×	✓	✓	×	×	18
Octodon degus	Degu	✓	✓	✓	×	×	×	×	×	×	18
Bathyergus suillus	Cape-dune mole rat	✓	✓	✓	×	×	×	×	×	×	21
Cryptomys hottentotus	Highveld mole rat	✓	✓	✓	×	×	×	×	×	×	21
Pedetes capensis	Springhare	✓	✓	✓	×	×	×	×	×	×	22
Anomalurus beecrofti	Beecroft's scaly-tailed squirrel	✓	✓	✓	×	×	×	×	×	×	22
Lagomorpha											
Lepus capensis	Cape hare	✓	✓	✓	×	×	×	×	×	×	23
Scandentia											
Tupaia belangeri	Northern tree shrew	✓	✓	✓	×	×	×	×	×	×	23
Primates											
Galago demidoff	Prince Demidoff's bushbaby	✓	✓	✓	×	×	×	×	×	×	24
Perodicticus potto	Potto	✓	✓	✓	×	×	×	×	×	×	24
Lemur catta	Ring-tailed lemur	✓	✓	✓	×	×	×	×	×	×	24
Macaca mulatta	Rhesus macaque	✓	✓	✓	×	×	×	×	×	×	25
Hylobates lar	Lar gibbon	✓	✓	✓	✓	×	×	×	×	×	26
Pan troglodytes	Chimpanzee	✓	✓	✓	✓	×	×	×	×	×	26
Homo sapiens	Human	✓	✓	✓	×	×	×	×	×	×	27, 28
Macroscelidea											
Petrodromus tetradactylus	Four-toed sengi	✓	✓	✓	×	×	×	×	×	×	29
Afrosoricida											

(Continues)

TABLE 3 (Continued)

Clade/Order/*Genus species*	Common name	Orexinergic neuronal populations/clusters									Source
		Mc	Zic	OTc	SO	Pc	PAH	SON	RChL	ME	
Amblysomus hottentotus	Hottentot golden mole	✓	✓	✓	×	×	×	×	×	×	29
Potomogale velox	Giant otter shrew	✓	✓	✓	×	×	×	×	×	×	29
Hyrocoidea											
Procavia capensis	Rock hyrax	✓	✓	✓	×	×	×	×	×	×	30
Proboscidea											
Loxodonta africana	African elephant	✓	✓	✓	×	✓	×	×	×	×	31

Note: Color coding: gray cells indicate nuclei typically present (✓) or absent (×); green cells represent putative novel additional nuclei not found in other species; red cells represent putative loss of specific nuclei typically present in other species.

Abbreviations: Mc, main orexinergic cluster; ME, potential median eminence orexinergic cells (tanycytes and macrophages); OTc, optic tract orexinergic cluster; PAH, potential paraventricular hypothalamic nucleus orexinergic cluster; Pc, parvocellular orexinergic cluster; RChL, potential lateral part of the retrochiasmatic area orexinergic cluster; SO, potential supraoptic orexinergic cluster; SON, potential supraoptic nucleus orexinergic cluster; Zic, zona incerta orexinergic cluster.

Sources of data: (1) Yamamoto et al. (2006); (2) Patzke et al. (2014); (3) Imam et al. (2019); (4) Pillay et al. (2017); (5) Thannickal, Nienhuis, et al. (2000); (6) Wagner et al. (2000) and Zhang et al. (2001); (7) current study; (8) Kruger et al. (2010); (9) Dell et al. (2013); (10) Calvey et al. (2016); (11) Dell et al. (2012); (12) Davimes et al. (2017); (13) Malungo et al. (2020); (14) Iqbal et al. (2001); (15) Dell, Patzke, et al. (2016); (16) Dell, Karlsson, et al. (2016); (17) Ettrup et al. (2010); (18) Nixon and Smale (2007); (19) Chen et al. (1999); (20) Kruger et al. (2012); (21) Bhagwandin et al. (2011); (22) Sweigers et al. (2017); (23) Calvey, Alagaili, et al. (2015); (24) Calvey, Patzke, et al. (2015); (25) Luna et al. (2017); (26) Williams et al. (2022); (27) Thannickal, Moore, et al. (2000); (28) Moore et al. (2001); (29) Calvey et al. (2013); (30) Gravett et al. (2011); and (31) Maseko et al. (2013).

cluster. The parvocellular orexinergic neurons, due to their much smaller soma volume and location medial to the main orexinergic cluster, formed a distinct and readily identifiable orexinergic cluster in the felids studied. The parvocellular orexinergic cluster has not been observed in other, smaller carnivores (Table 3; Pillay et al., 2017; Thannickal et al., 2000; Wagner et al., 2000; Zhang et al., 2001), and is not present in most mammals previously studied (Table 3). Parvocellular orexinergic neurons were first described in the hypothalami of the giraffe and harbor porpoise (Dell et al., 2012), with similar observations in other species of Cetartiodactyla (Davimes et al., 2017; Dell et al., 2012; Dell, Karlsson, et al., 2016; Dell, Patzke, et al., 2016; Ettrup et al., 2010; Iqbal et al., 2001; Malungo et al., 2020) and the African elephant (Maseko et al., 2013).

Until the current report revealing the parvocellular orexinergic cluster within the three felids studied, this parvocellular cluster had only been observed in mammalian species that ingest large volumes of plant matter that are low in calorie content (or large volumes of high calorie content food in the case of cetaceans). These observations suggested that the parvocellular orexinergic neurons may play a role in increasing the time spent awake (arousal) allowing the animals to obtain adequate nutrition (satiety) (e.g., Malungo et al., 2020); however, this argument cannot be extended to the felids studied, as they typically hunt/eat high-calorie food every 2–5 days (Skinner & Chimimba, 2005). Thus, the Cetartiodactyla with their consistent daily high food intake contrasts with the irregular food intake of the larger felids, yet the parvocellular orexinergic cluster is present. The smaller carnivores, where the parvocellular orexinergic cluster has not been reported (Table 3), typically eat on a daily basis (e.g., Skinner & Chimimba, 2005). Thus, speculatively, the presence of the parvocellular orexinergic cluster in the sporadically eating larger carnivores may establish the arousal

threshold required for these species to initiate hunting. Determining the presence or absence of the parvocellular orexinergic cluster in further mammal species, such as the Perissodactyla, other larger and smaller Carnivora, and Carnivora that have an exclusively herbivorous diet such as the giant and red panda, may provide clues regarding the potential function of this atypical orexinergic nucleus.

4.4 | Potential additional orexinergic neuron clusters in the Asiatic and African lions

In the Asiatic and African lions studied, but not the Southeast African cheetah, neurons appearing to be immunopositive for the orexin-A antibody used were observed in the paraventricular hypothalamic nucleus, supraoptic nucleus, and the lateral part of the retrochiasmatic area. In addition, in the two lions, what appear to be tanycytes and macrophages within the inner layer of the median eminence also appeared to show distinct immunopositivity. These potentially orexinergic neurons (and other cell types) are typically not reported in mammals (Table 3); however, similar patterns of neuronal staining with an orexin antibody were observed in the paraventricular hypothalamic nucleus and supraoptic nucleus in the Long–Evans strain of laboratory rat, the Golden hamster, and the Nile grass rat (Nixon & Smale, 2007). In addition, orexinergic immunopositive neurons have been reported in the median eminence of the Sprague–Dawley strain of laboratory rat (Chen et al., 1999), although this differs significantly from the potentially immunopositive tanycytes and macrophages observed in the lions examined in the current study.

These additional sites of orexin immunoreactivity may be false positives due to nonspecific binding of the rabbit polyclonal orexin-A antibody used in this study, as there are no reports of the presence

of *prepro-orexin* mRNA in these regions of the rat hypothalamus (Soya & Sakurai, 2020). This contrasts with the presence of orexin genes in the ventromedial supraoptic region in humans (Krolewski et al., 2010), which correlates with the presence of orexinergic neurons in this region in the lar gibbon, chimpanzee (Williams et al., 2022), and the three felids in the current study. Alternatively, as suggested by Nixon and Smale (2007), these additional neurons/cells may actively uptake orexin produced by neurons in other parts of the hypothalamus, as orexinergic immunopositive axons are present in these regions (e.g., Figures 8d,f and 10d,f). It is possible that while the larger boutons observed as part of the orexinergic axons communicate through synaptic transmission, the smaller orexinergic boutons may secrete orexin for volume transmission communication (Dell et al., 2015), thereby allowing the potential substrate for the uptake of the orexin molecule by the neurons/cells in these regions not typically observed to be orexinergic in the mammalian hypothalamus. Thus, there remains the potential that at least in some species, the orexinergic system is far more complex than typically observed.

4.5 | Complexity of the orexinergic system in mammals

The current study, along with those of 51 other mammal species/strains (Table 3 and references therein), indicates that typically the mammalian orexinergic neurons are found within three clusters restricted to the hypothalamus, the main, zona incerta, and optic tract clusters. Despite this consistency, there are indications of variations in the organization of this system. The current study of the felids, along with that of the lar gibbon and chimpanzee (Williams et al., 2022), indicates that one variation is the presence of orexinergic neurons in the ventromedial supraoptic hypothalamus, which we term the supraoptic orexinergic cluster. The second variation of significance is the presence of the distinct parvocellular orexinergic cluster in the Cetartiodactyls, African elephant, and the three felids studied herein (Table 3). Both of these variations have now been reported in mammal species that can be considered members of distinct phylogenetic lineages, which indicates that the activation and expression of orexin genes leading to the production of the orexin molecule have the potential to occur in at least two regions outside of the locations where orexinergic neurons are typically observed. In the lions and some species/strains of rodents, further potential neuronal clusters for the production of orexin have also been revealed, although these require further investigation for validation or negation. It can be proposed that further studies of the orexinergic system across more mammalian species, including lineages such as the monotremes, perissodactyls, and xenarthrans among others, may reveal additional variations in the organization of the neurons that produce orexin and influence whole organism behaviors such as sleep and the acquisition of nutrition.

AUTHOR CONTRIBUTIONS

Demi Oddes, Ayanda Ngwenya, Illke B. Malungo, and Paul R. Manger conceptualized the study. Anita Burkevica, Therese Hård, and Mads F.

CONFLICT OF INTEREST

The authors declare no conflict of interest.

DATA AVAILABILITY STATEMENT

Data have not been shared due to this study being based on histological sections.

ORCID

Muhammad A. Spocter https://orcid.org/0000-0003-1174-7444
Paul R. Manger https://orcid.org/0000-0002-1881-2854

PEER REVIEW

The peer review history for this article is available at https://publons.com/publon/10.1002/cne.25431.

REFERENCES

Bertelsen, M. F. (2018). Issues surrounding surplus animals in zoos. In R. E. Miller, N. Lamberski, & P. Calle (Eds.), *Fowler's zoo and wild animal medicine, current therapy* (Vol. 9, pp. 134–137). Elsevier.

Bhagwandin, A., Fuxe, K., Bennett, N. C., & Manger, P. R. (2011). Distribution of orexinergic neurons and their terminal networks in the brains of two species of African mole rats. *Journal of Chemical Neuroanatomy*, *41*, 32–42. https://doi.org/10.1016/j.jchemneu.2010.11.002

Bininda-Emonds, O. R. P., Gittleman, J. L., & Purvis, A. (1999). Building large trees by combining phylogenetic information: A complete phylogeny of the extant Carnivora (Mammalia). *Biological Reviews of the Cambridge Philosophical Society*, *74*, 143–175. https://doi.org/10.1017/s00063231999005307

Calvey, T., Patzke, N., Kaswera, C., Gilissen, E., Bennett, N. C., & Manger, P. R. (2013). Nuclear organisation of some immunohistochemically identifiable neural systems in three Afrotherian species – *Potomogale velox*, *Amblysomus hottentotus* and *Petrodromus tetradactylus*. *Journal of Chemical Neuroanatomy*, *50–51*, 48–65. https://doi.org/10.1016/j.jchemneu.2013.01.002

Calvey, T., Alagaili, A. N., Bertelsen, M. F., Bhagwandin, A., Pettigrew, J. D., & Manger, P. R. (2015). Nuclear organisation of some immunohistochemically identifiable neural systems in two species of the Euarchontoglires: A Lagomorph, *Lepus capensis*, and a Scandentia, *Tupaia belangeri*. *Journal of Chemical Neuroanatomy*, *70*, 1–19. https://doi.org/10.1016/j.jchemneu.2015.10.007

Calvey, T., Patzke, N., Kaswera-Kyamakya, C., Gilissen, E., Bertelsen, M. F., Pettigrew, J. D., & Manger, P. R. (2015). Organization of cholinergic, catecholaminergic, serotonergic and orexinergic nuclei in three strepsirrhine primates: *Galago demidoff*, *Perodicticus potto* and *Lemur catta*. *Journal of Chemical Neuroanatomy*, *70*, 42–57. https://doi.org/10.1016/j.jchemneu.2015.10.002

Calvey, T., Patzke, N., Bennett, N. C., Kaswera-Kyamakya, C., Gilissen, E., Alagaili, A. N., Mohammed, O. B., Pettigrew, J. D., & Manger, P. R. (2016). Nuclear organisation of some immunohistochemically identifiable neural systems in five species of insectivore – *Crocidura cyanea*, *Crocidura olivieri*, *Sylvisorex ollula*, *Paraechinus aethiopicus* and *Atelerix frontalis*. *Journal of Chemical Neuroanatomy*, *72*, 34–52. https://doi.org/10.1016/j.jchemneu.2015.12.012

Chen, C. T., Dun, S. L., Kwok, E. H., Dun, N. J., & Chang, J. K. (1999). Orexin A-like immunoreactivity in the rat brain. *Neuroscience Letters*, *260*, 161–164. https://doi.org/10.1016/s0304-3940(98)00977-x

Davimes, J. G., Alagaili, A. N., Bennett, N. C., Mohammed, O. R., Bhagwandin, A., Manger, P. R., & Gravett, N. (2017). Neurochemical organization and morphology of the sleep related nuclei in the brain of the Arabian oryx, *Oryx leucoryx*. *Journal of Chemical Neuroanatomy*, *81*, 53–70. https://doi.org/10.1016/j.jchemneu.2017.02.002

de Lecea, L., Kilduff, T. S., Peyron, C., Gao, X., Foye, P. E., Danielson, P. E., Fukuhara, C., Battenberg, E. L., Gautvik, V. T., Bartlett, F. S., Frankel, W. N., van den Pol, A. N., Bloom, F. E., Gautvik, K. M., & Sutcliffe, J. G. (1998). The hypocretins: Hypothalamus-specific peptides with neuroexcitatory activity. *Proceedings of the National Academy of Sciences of the United States of America*, *95*, 322–327. https://doi.org/10.1073/pnas.95.1.322

Dell, L. A., Patzke, N., Bhagwandin, A., Bux, F., Fuxe, K., Barber, G., Siegel, J. M., & Manger, P. R. (2012). Organization and number of orexinergic neurons in the hypothalamus of two species of Cetartiodactyla: A comparison of giraffe (*Giraffe camelopardalis*) and harbour porpoise (*Phocoena phocoena*). *Journal of Chemical Neuroanatomy*, *44*, 98–109. https://doi.org/10.1016/j/jchemneu.2012.06.001

Dell, L. A., Kruger, J. L., Pettigrew, J. D., & Manger, P. R. (2013). Cellular location and major terminal networks of the orexinergic system in the brain of two megachiropterans. *Journal of Chemical Neuroanatomy*, *53*, 64–71. https://doi.org/10.1016/j.jchemneu.2013.09.001

Dell, L. A., Spocter, M. A., Patzke, N., Karlson, K. A., Alagaili, A. N., Bennett, N. C., Muhammed, O. B., Bertelsen, M. F., Siegel, J. M., & Manger, P. R. (2015). Orexinergic bouton density is lower in the cerebral cortex of cetaceans compared to artiodactyls. *Journal of Chemical Neuroanatomy*, *68*, 61–76. https://doi.org/10.1016/j.jchemneu.2015-07.007

Dell, L. A., Karlsson, K. A., Patzke, N., Spocter, M. A., Siegel, J. M., & Manger, P. R. (2016). Organization of the sleep-related neural systems in the brain of the minke whale (*Balaenoptera acutorostrata*). *Journal of Comparative Neurology*, *524*, 2018–2035. https://doi.org/10.1002/cne.23931

Dell, L. A., Patzke, N., Spocter, M. A., Bertelsen, M. F., Siegel, J. M., & Manger, P. R. (2016). Organization of the sleep-related neural systems in the brain of the river hippopotamus (*Hippopotamus amphibius*). *Journal of Comparative Neurology*, *524*, 2036–2058. https://doi.org/10.1002/cne.23930

Ettrup, K. S., Sørensen, J. S., & Bjarkam, C. R. (2010). The anatomy of the Göttingen minipig hypothalamus. *Journal of Chemical Neuroanatomy*, *39*, 151–165. https://doi.org/10.1016/j.jchemneu.2009.12.004

Gravett, N., Bhagwandin, A., Fuxe, K., & Manger, P. R. (2011). Distribution of orexin-A immunoreactive neurons and their terminal networks in the brain of the rock hyrax, *Procavia capensis*. *Journal of Chemical Neuroanatomy*, *41*, 86–96. https://j.jchemneu.2010.11.005

Gundersen, H. J. (1988). The nucleator. *Journal of Microscopy - Oxford*, *151*, 3–21. https://doi.org/10.1111/j.1365-2818.1988.tb04609.x

Imam, A., Bhagwandin, A., Ajao, M. S., & Manger, P. R. (2019). The brain of the tree pangolin (*Manis tricuspis*). V. The diencephalon and hypothalamus. *Journal of Comparative Neurology*, *527*, 2413–2439. https://doi.org/10.1002/cne.24619

Inutsuka, A., & Yamanaka, A. (2013). The regulation of sleep and wakefulness by the hypothalamic neuropeptide orexin/hypocretin. *Nagoya Journal of Medical Science*, *75*, 29–36.

Iqbal, J., Pompolo, S., Sakurai, T., & Clarke, I. J. (2001). Evidence that orexin-containing neurons provide direct input to gonadotrophin-releasing hormone neurones in the ovine hypothalamus. *Journal of Neuroendocrinology*, *13*, 1033–1041. https://doi.org/10.1046/j.1365-2826.2001.00719.x

Krolewski, D. M., Medina, A., Kerman, I. A., Bernard, R., Burker, S., Thompson, R. C., Bunney, W. E. Jr, Schatzberg, A. F., Myers, R. M., Akil, H., Jones, E. G., & Watson, S. J. (2010). Expression patterns of corticotropin-releasing factor, arginine vasopressin, histidine decarboxylase, melanin-concentrating hormone, and orexin genes in the human hypothalamus. *Journal of Comparative Neurology*, *518*, 4591–4611. https://doi.org/10.1002/cne.22480

Kruger, J. L., Dell, L. A., Pettigrew, J. D., & Manger, P. R. (2010). Cellular location and major terminal networks of the orexinergic system in the brains of five microchiropteran species. *Journal of Chemical Neuroanatomy*, *40*, 256–262. https://doi.org/10.1016/j.jchemneu.2010.07.004

Kruger, J. L., Patzke, N., Fuxe, K., Bennett, N. C., & Manger, P. R. (2012). Nuclear organization of cholinergic, putative catecholaminergic, serotonergic and orexinergic systems in the brain of the African pygmy mouse (*Mus minutoides*): Organizational complexity is preserved in small brains. *Journal of Chemical Neuroanatomy*, *44*, 45–56. https://doi.org/10.1016/j.jchemneu.2012.04.002

Kukkonen, J. P., Holmqvist, T., Ammoun, S., & Åkerman, K. E. O. (2002). Functions of the orexinergic/hypocretinergic system. *American Journal of Physiology – Cell Physiology*, *283*, C1567–C1591. https://doi.org/10.1152/ajpcell.00055.2002

Li, S., & Kiruoac, J. (2008). Projections from the paraventricular nucleus of the thalamus to the forebrain, with special emphasis on the extended amygdala. *Journal of Comparative Neurology*, *506*, 263–287. https://doi.org/10.1002/cne.21502

Luna, S. L., Brown, D. I., Eghlidi, D. H., Kohama, S. G., & Urbanski, H. F. (2017). Locomotor activity and the expression of orexin A and orexin B in aged female rhesus macaques. *Neurobiology of Aging*, *50*, 1–4. https://doi.org/10.1016/j.neurobiolaging.2016.10.016

Manger, P. R., Pillay, P., Maseko, B. C., Bhagwandin, A., Gravett, N., Moon, D. J., Jillani, N., & Hemingway, J. (2009). Acquisition of brains from the African elephant (*Loxodonta africana*): Perfusion-fixation and dissection. *Journal of Neuroscience Methods*, *179*, 16–21. https://doi.org/10.1016/j/jneumeth.2009.01.001

Malungo, I. B., Gravett, N., Bhagwandin, A., Davimes, J. G., & Manger, P. R. (2020). A preliminary description of the sleep-related neural systems in the brain of the blue wildebeest, *Connochaetes taurinus*. *The Anatomical Record*, *303*, 1977–1997. https://doi.org/10.1002/ar.24265

Maseko, B. C., Patzke, N., Fuxe, K., & Manger, P. R. (2013). Architectural organization of the African elephant diencephalon and brainstem. *Brain, Behavior and Evolution*, *82*, 83–128. https://doi.org/10.1159/000352004

Moore, R. Y., Abrahamson, E. A., & van den Pol, A. (2001). The hypocretin neuron system: An arousal system in the human brain. *Archives Italiennes Biologie*, *139*, 195–205.

Nambu, T., Sakurai, T., Mizukami, K., Hosoya, Y., Yanagisawa, M., & Goto, K. (1999). Distribution of orexin neurons in the adult rat brain. *Brain Research*, *827*, 243–260. https://doi.org/10.1016/S0006-8993(99)01336-0

Nixon, J. P., & Smale, L. (2007). A comparative analysis of the distribution of immunoreactive orexin A and B in the brains of nocturnal and diurnal rodents. *Behavioral and Brain Functions*, *3*, 28. https://doi.org/10.1186/1744-9081-3-28

Patzke, N., Bertelsen, M. F., Fuxe, K., & Manger, P. R. (2014). Nuclear organization of cholinergic, catecholaminergic, serotonergic and orexinergic systems in the brain of the Tasmanian devil (*Sarcophilus harrisii*). *Journal of Chemical Neuroanatomy*, *61–62*, 94–106. https://doi.org/10.1016/j.jchemneu.2014.08.005

Peyron, C., Tighe, D. K., van den Pol, A. N., de Lecea, L., Heller, H. C., Sutcliffe, J. G., & Kilduff, T. S. (1998). Neurons containing hypocretin (orexin) project to multiple neuronal systems. *Journal of Neuroscience*, *18*, 9996–10015. https://doi.org/10.1523/JNEUROSCI.18-23-09996.1998

Pillay, S., Bhagwandin, A., Bertelsen, M. F., Patzke, N., Engler, G., Engel, A. K., & Manger, P. R. (2017). Regional distribution of cholinergic, catecholaminergic, serotonergic and orexinergic neurons in the brain of two carnivore species: The feliform banded mongoose (*Mungos mungo*) and

the caniform domestic ferret (*Mustella putorius furo*). *Journal of Chemical Neuroanatomy*, *82*, 12–28. https://doi.org/10.1016/j.jchemneu.2017.04.001

Pop, M. G., Crivii, C., & Opincariu, I. (2018). Chapter 1. Anatomy and function of the hypothalamus. In (S. Baloyannis & J. Gordeladze Eds.), *The hypothalamus in health and disease* (pp. 3–14). IntechOpen. https://doi.org/10.5772/intechopen.80728

Sakurai, T., Amemiya, A., Ishii, M., Matsuzaki, I., Chemelli, R. M., Tanaka, H., Williams, S. C., Richardson, J. A., Kozlowski, G. P., Wilson, S., Arch, J. R., Buckingham, R. E., Haynes, A. C., Carr, S. A., Annan, R. S., McNulty, D. E., Liu, W. S., Terrett, J. A., Elshourbagy, N. A., … Yanagisawa, M. (1998). Orexins and orexin receptors: A family of hypothalamic neuropeptides and G protein-coupled receptors that regulate feeding behavior. *Cell*, *92*, 573–585. https://doi.org/10.1016/S0092-8674(00)80949-6

Skinner, J. D., & Chimimba, C. T. (2005). *The mammals of the southern African subregion* (3rd ed.). Cambridge University Press.

Soya, S., & Sakurai, T. (2020). Evolution of orexin neuropeptide system: Structure and function. *Frontiers in Neuroscience*, *14*, 691. https://doi.org/10.3389/fnins.2020.00691

Sweigers, J., Bhagwandin, A., Spocter, M. A., Kaswera-Kyamakya, C., Gilissen, E., Manger, P. R., & Maseko, B. C. (2017). Nuclear organisation of cholinergic, catecholaminergic, serotonergic and orexinergic neurons in two relatively large-brained rodent species – The springhare (*Pedetes capensis*) and Beecroft's scaly-tailed squirrel (*Anomalurus beecrofti*). *Journal of Chemical Neuroanatomy*, *86*, 78–91. https://doi.org/10.1016/j.jchemneu.2017.09.002

Thannickal, T. C., Nienhuis, R., Ramanathan, L., Gulyani, S., Turner, K., Chestnut, B., & Siegel, J. M. (2000). Preservation of hypocretin neurons in genetically narcoleptic dogs. *Sleep*, *23*, A296–A296.

Thannickal, T. C., Moore, R. Y., Nienhuis, R., Ramanathan, L., Gulyani, S., Aldrich, M., Cornford, M., & Siegel, J. M. (2000). Reduced number of hypocretin neurons in human narcolepsy. *Neuron*, *27*, 469–474. https://doi.org/10.1016/s0896-6273(00)00058-1

Wagner, D., Salin-Pascual, R., Greco, M. A., & Shiromani, P. J. (2000). Distribution of hypocretin-containing neurons in the lateral hypothalamus and c-Fos-immunoreactive neurons in the VLPO. *Sleep Research Online*, *3*, 35–42.

West, M. J., Slomianka, L., & Gundersen, H. J. (1991). Unbiased stereological estimation of the total number of neurons in the subdivisions of the rat hippocampus using the optical fractionator. *Anatomical Record*, *231*, 482–497. https://doi.org/10.1002/ar.1092310411

Williams, V. M., Bhagwandin, A., Swiegers, J., Bertelsen, M. F., Hård, T., Thannickal, T. C., Siegel, J. M., Sherwood, C. C., & Manger, P. R. (2022). Nuclear organization of orexinergic neurons in the hypothalamus of a lar gibbon and a chimpanzee. *The Anatomical Record*, *305*, 1459–1475. https://doi.org/10.1002/ar24775

Yamamoto, Y., McKinley, M. J., Nakazato, M., Yamashita, H., Shirahata, A., & Ueta, Y. (2006). Postnatal development of orexin-A and orexin-B like immunoreactivities in the Eastern grey kangaroo (*Macropus giganteus*) hypothalamus. *Neuroscience Letters*, *392*, 124–128. https://doi.org/10.1016/j.neulet.2005.09.014

Zhang, J. H., Sampogna, S., Morales, F. R., & Chase, M. H. (2001). Orexin (hypocretin)-like immunoreactivity in the cat hypothalamus: A light and electron microscope study. *Sleep*, *24*, 67–76. https://doi.org/10.1093/sleep/24.1.67

Zhang, X. Y., Yu, L., Zhuang, Q. X., Zhu, J. N., & Wang, J. J. (2013). Central functions of the orexinergic system. *Neuroscience Bulletin*, *29*, 355–365. https://doi.org/10.1007/s12264-012-1297-4